3-2009

Synthesis and Evaluation of Lanthanide Ion DOTA-tetraamide Complexes bearing Peripheral Hydroxyl Groups

Azhar Pasha
University of Texas at Dallas

Mai Lin
University of Texas Southwestern Medical Center

Gyula Tircso
University of Texas at Dallas

Cynthia L. Rostollan
University of Texas Southwestern Medical Center

Mark Woods
Portland State University, mark.woods@pdx.edu

See next page for additional authors

Citation Details

Pasha, A., Lin, M., Tircsó, G., Rostollan, C. L., Woods, M., Kiefer, G. E., ... & Sun, X. (2009). Synthesis and evaluation of lanthanide ion DOTA–tetraamide complexes bearing peripheral hydroxyl groups. JBIC Journal of Biological Inorganic Chemistry, 14(3), 421-438.

Published in final edited form as:
J Biol Inorg Chem. 2009 March ; 14(3): 421–438. doi:10.1007/s00775-008-0459-3.

Synthesis and evaluation of lanthanide ion DOTA-tetraamide complexes bearing peripheral hydroxyl groups

Azhar Pasha[1], **Mai Lin**[2], **Gyula Tircsó**[1,3], **Cynthia L. Rostollan**[2], **Mark Woods**[1,4], **Garry E. Kiefer**[1,4,*], **A. Dean Sherry**[1,5,*], and **Xiankai Sun**[2,*]

[1]Department of Chemistry, University of Texas at Dallas, P.O. Box 803066, Richardson, TX 75083, USA

[2]Department of Radiology, University of Texas Southwestern Medical Center, 5323 Harry Hines Blvd, Dallas, TX 75390-8542, USA

[3]Department of Inorganic and Analytical Chemistry, University of Debrecen, Egyetem ter 1, P.f. 21, Debrecen, H-4010, Hungary

[4]Macrocyclics, 2110 Research Row, Suite 425, Dallas, TX, 75235, USA

[5]Advanced Imaging Research Center, University of Texas Southwestern Medical Center, 5323 Harry Hines Blvd, NE 4.2, Dallas, TX 75390-8568, USA

Abstract

The use of lanthanide-based contrast agents for magnetic resonance imaging (MRI) has become an integral component of this important diagnostic modality. These inert chelates typically possess high thermodynamic stability constants that serve as a predictor for *in vivo* stability and low toxicity. Recently a new class of contrast agents was reported having a significantly lower degree thermodynamic stability while exhibiting biodistribution profiles indicative of high stability under biological conditions. These observations are suggestive that the nature of contrast agent stability is also dependent upon the kinetics of complex dissociation; a feature of potential importance when contemplating the design of new chelates for *in vivo* use. In this paper we present a study of the kinetics of acid catalyzed dissociation, thermodynamic stability, serum stability and biodistribution of a series of DOTA-tetraamide complexes that have been substituted with peripheral hydroxyl groups. The data indicate that these non-traditional contrast agents exhibit *in vivo* stability comparable to agents with much higher log K_{ML} values demonstrating the important contribution of kinetic inertness.

Keywords

Biodistribution; Toxicity; Lanthanides complexes; DOTA-tetraamide derivatives; MRI contrast agents; Lutetium-177

Introduction

Magnetic resonance imaging (MRI) has become one of the most powerful non-invasive tools for modern diagnostic medicine. To a large extent, growth and acceptance of this modality have been strongly influenced by the use of paramagnetic contrast agents which enhance image

*Garry E. Kiefer, Garry@macrocyclics.com, Fax: 972-250-2245. *A. Dean Sherry, Dean.Sherry@UTSouthwestern.edu, sherry@utdallas.edu, Fax: 214-645-2744. *Xiankai Sun, Xiankai.Sun@UTSouthwestern.edu, Fax: 214-645-2885.

quality and soft tissue delineation thus providing additional information for a more rapid and accurate diagnosis [1,2]. For this purpose gadolinium chelates have proven to be the most versatile family of contrast agent owing to their high spin state and long electronic relaxation times which reduce the relaxation rate of water protons in tissue resulting in enhanced image contrast. The primary mechanism of relaxation by gadolinium-based magneto-pharmaceutical agents is dependent upon the rapid exchange of metal-coordinated water molecules with surrounding bulk water which then generates a higher contrast image due to the shorter relaxation times of the bulk water.

Equally important to MR contrast agent development has been the refinement of ligand structures needed to effectively render the lanthanide ion non-toxic. A variety of both acyclic and cyclic ligand frameworks are frequently employed for imaging modalities, each having unique properties that can be adapted to meet the requirements of a specific application (Chart 1). Despite certain structural variations, these ligand systems all possess the common features necessary for generating stable complexes for *in vivo* use; i.e. the familiar octadentate coordination geometry and neutral or anionic charge imparted by the polyamino-carboxylate ligand framework. This signature coordination geometry is present in both the linear and macrocyclic structures best exemplified by the workhorse ligands, DTPA and DOTA. Over the years these two ligands have served as the foundation for nearly all medical applications of lanthanide ions; a consequence of their unsurpassed chelation properties. Ultimately these collective traits afford proven drug formulations that are non-toxic at the necessary dosage levels and exhibit very efficient renal clearance profiles for all current MR contrast agents.

An exciting new development in the field of contrast agents has been the discovery that certain types of paramagnetic chelates with moderate water exchange rates can be used to generate contrast enhancement by an entirely different mechanism [3]. Unlike their predecessors these new contrast agents make possible the selective pre-saturation of the bound water molecule due to slower water exchange kinetics. Once saturated, the bound water molecule then exchanges (no longer coordinated to the metal) becoming part of the surrounding water pool where it transfers the saturation effect to neighbouring water protons. The net result is that diminished image intensity is observed in regions of that contain contrast agent. Large lanthanide induced chemical shifts of the bound water protons alleviate the problems of direct saturation of the solvent water while permitting more rapid saturation transfer. The process of altering proton signal intensity *via* selective presaturation of a neighbouring pool of protons is commonly referred to as CEST (Chemical Exchange Saturation Transfer) and when CEST is produced by a paramagnetic chelate the effect is referred to as PARACEST.

The general structure of PARACEST contrast agents is strikingly similar to that of the macrocyclic conventional MR agents GdDOTA and its analogues GdHPDO3A and GdDO3A-butrol (Chart1). Two major structural differences exist between these PARACEST agents and their conventional counterparts. First, the central gadolinium ion is replaced by a paramagnetic lanthanide ion with an anisotropic f-electron shell that can induce significant hyperfine shifts in neighbouring protons. Europium(III) is a common choice for PARACEST applications. Second, the carboxylate pendant arms of the ligand are replaced by amide ligands and this modulates the water exchange rate such that it is amenable for CEST applications. In addition, the amide substituent may be modified in such a way that further fine tuning of water exchange kinetics is possible [4]. These changes in the nature of coordinate bonding with the metal ion have been found to exert an important influence over the kinetics of dissociation [5], thermodynamic stability [5–7] and physiological tolerance [8]. Our interest in CEST imaging using PARACEST agents has prompted an effort to refine this class of chelate with a view to *in vivo* applications. Of particular interest has been the effect that the nature of the amide substituent plays in controlling the magnitude of CEST and the physiological tolerance of these chelates. Stimulated by the idea that both the CEST properties and the *in vivo* tolerance may

be improved by incorporating a large number of hydroxyl groups into the complex, we prepared and studied a series of derivatized chelates containing four (L^4), eight (L^8) and twelve (L^{12}) hydroxyl groups (Chart 2). The CEST properties of EuL^4, EuL^8 and EuL^{12} will be reported in a companion paper [9]. Each complex was found to exhibit a PARACEST effect arising from the coordinated water molecule but no CEST, or CEST enhancement, was observed arising from the peripheral hydroxyl groups. In this paper we examine the in vitro stability as well as the biodistribution profiles of this new class of PARACEST agent.

Materials and Methods

General Remarks

All chemicals were obtained from commercial sources and used without further purification unless otherwise stated. All solvents were of HPLC grade and used as received unless otherwise stated. Water refers to deionized water with a specific resistance of 18 $M\Omega cm^{-1}$. The ^1H and ^{13}C NMR spectra were recorded on a JEOL Eclipse 270 MHz spectrometer operating at 270 MHz. Chemical shifts are reported in parts per million (δ) and referenced to TMS. Infrared spectra were recorded on a Nicolet Avatar 360 FT-IR spectrometer as KBr pellets, UV-Vis absorption spectra and kinetics were recorded using Cary 300 Bio UV-Vis spectrophotometer. Electrospray ionization mass spectrometry (ESI-MS) was performed by HT Laboratories, San Diego, California. Elemental analyses were performed by the Micro Laboratory, University of Illinois at Urbana Champaign. Radio-thin layer chromatography (TLC) analysis was performed on a Rita Star Radioisotope TLC Analyzer (Straubenhardt, Germany).

Synthesis of Ligands

***N-tert*-Butyloxycarbonyl-tris hydroxymethyl-aminomethane (4)—**A solution of di-*tert*-butyl dicarbonate (46.0 g, 215.0 mmol) in *tert*-butnaol (150 mL) was added to a suspension of trishydroxymethyl aminomethane **1** (20.0 g, 165.0 mmol) in 1:1 (v:v) mixture of methanol and *tert*-butanol (250 mL). The mixture was stirred at room temperature for 18 h. The solvents were then removed under reduced pressure and the residue purified by trituration with cold ethyl acetate. The title compound was isolated by vacuum filtration as a colourless solid (35.0 g, 96%). ^1H NMR (270 MHz, DMSO-d_6) δ = 5.75 (1H, s br, NH), 4.51 (3H, s br, OH), 3.51 (6H, s, $C(CH_2OH)_3$), 1.36 (9H, s, (CH_3)); ^{13}C NMR (67.5 MHz, DMSO-d_6) δ = 155.6 (C=O), 78.4 ($C(CH_3)_3$), 61.0 (CH_2OH), 60.8 (CCH_2OH), 28.8 (CH_3); *m/z* (ESI+) 222 (100%, $[M+H]^+$), 244 (50%, $[M+Na]^+$); ν_{max} / cm^{-1} (thin film): 3304 (NH), 3062, 2962, 2878, 1679 (C=O), 1550, 1467, 1370, 1294, 1167, 1120, 1074, 1016, 871 and 720.

***tert*-Butyl-2-(benzyloxy)ethyl carbamate (5)—**A solution of *N*-Boc-ethanolamine **2** (20.0 g, 124.0 mmol) and benzyl bromide (22.1 mL, 186.0 mmol) in anhydrous dichloromethane (200 mL) was stirred at 0 °C under argon. Portions of finely ground potassium hydroxide (10.4 g, 186.0 mmol) were added over a period of 30 min. After addition was complete the mixture was stirred at room temperature for 18 h. The solvents were then removed under reduced pressure and the residue taken up into dichloromethane (200 mL) and water (200 mL). The two layers were separated and the aqueous layer extracted with CH_2Cl_2 (3 × 20 mL). The combined organic layers were dried (Na_2SO_4) and the solvents removed under reduced pressure. The oily residue was purified by column chromatography over silica gel eluting with hexane, followed by 5% EtOAc in hexane to afford the title compound as a colourless oil (21.8 g, 70%). R_f = 0.12 (5% EtOAc in CH_2Cl_2, SiO_2); ^1H NMR (270 MHz, $CDCl_3$) δ = 7.31 (5H, m, Ar), 4.97 (1H, s,br, NH), 4.49 (2H, s, OCH_2Ar), 3.53 (2H, t, $^3J_{H\text{-}H}$ = 5 Hz, CH_2CH_2O), 3.34 (2H, qt, $^3J_{H\text{-}H}$ = 5 Hz $NHCH_2CH_2$), 1.42 (9H, s, CH_3); ^{13}C NMR (67.5 MHz, $CDCl_3$) δ = 156.1 (C=O), 138.1 (Ar), 128.5 (Ar), 127.8 (Ar), 79.3 ($C(CH_3)_3$), 73.1 (OCH_2Ar), 69.4 (CH_2CH_2O), 40.5 ($NHCH_2CH_2$), 28.5 (CH_3); ν_{max} / cm^{-1} (thin film): 3357 (NH), 2977, 2867, 1716 (C=O), 1521, 1366, 1250, 1171, 1098, 887, 739, 698.

***N-tert*-Butyl-(1,3-bisbenzyloxy)-2-propylcarbamate (6)—**The title compound was prepared according to the procedure used for compound **5** using *N-tert*-butyl-(3-benzyloxy)-2-amino-1-propanol **3** (20.0 g, 75.0 mmol), benzyl bromide (13.4 mL, 113.0 mmol) and potassium hydroxide (6.4 g, 113.0 mmol). The title compound was obtained as a colourless waxy solid (22.9 g, 86%). R_f = 0.15 (5% EtOAc in Hexane, SiO_2); ^{1}H NMR (270 MHz, DMSO-d_6) δ = 7.31 (5H, m, Ar), 6.77 (1H, d, $^3J_{H\text{-}H}$ = 8, NH), 4.46 (4H, s, OCH_2Ar), 3.86 (1H, ddd, $^3J_{H\text{-}H}$ = 7 Hz, $^3J_{H\text{-}H}$ = 7 Hz, $^3J_{H\text{-}H}$ = 6 Hz, NHCH$(CH_2)_2$), 3.44 (2H, d, $^3J_{H\text{-}H}$ = 7 Hz, CHCH_2O), 3.34 (2H, d, $^3J_{H\text{-}H}$ = 7 Hz, CH_2CH_2O), 1.38 (9H, s, CH_3); ^{13}C NMR (67.5 MHz, DMSO-d_6) δ = 155.9 (C=O), 139.0 (Ar), 128.7 (Ar), 128.0 (Ar), 78.3 (C$(CH_3)_3$), 72.6 (OCH_2Ar), 70.0 (CHCH_2O), 50.5 (NHCH$(CH_2)_2$), 28.8 (CH_3); *m/z* (ESI+) 372 (100%, $[M+H]^+$), 394 (60%, $[M+Na]^+$); ν_{max} / cm^{-1} (thin film): 2977, 2861, 2798, 1712 (C=O), 1496, 1453, 1363, 1248, 1170, 1103, 1027, 780, 737, 698, and 610.

***N-tert*-Butyloxycarbonyl-tris benzyloxymethyl-aminomethane (7)—**The title compound was prepared according to the procedure used for compound **5** using the BOC protected tris-hydroxy methyl aminomethane **4** (20 g, 90 mmol), benzyl bromide (70 mL, 589 mmol) and potassium hydroxide (81.4 g, 589 mmol). The title compound was obtained as a colourless oil (31.1 g, 68.0%). R_f = 0.19 (5% EtOAc in Hexane, SiO_2); ^{1}H NMR (270 MHz, $CDCl_3$) δ = 7.37 (5H, m, Ar), 5.11 (1H, s, NH), 4.57 [6H, s, $(OCH_2Ar)_3$], 3.88 (6H, s, C$(CH_2O)_3$), 1.50 (9H, s, CH_3); ^{13}C NMR (67.5 MHz, $CDCl_3$) δ = 155.0 (C=O), 138.5 (Ar), 128.5 (Ar), 127.7 (Ar), 79.2 (C$(CH_3)_3$), 73.5 (OCH_2Ar), 69.7 [C$(CH_2O)_3$], 58.9 (NHCCH_2O), 28.6 (CH_3); *m/z* (ESI+) 492 (100%, $[M+H]^+$), 514 (100%, $[M+Na]^+$); ν_{max} / cm^{-1} (thin film): 3442 (NH), 2917, 2835, 1720 (C=O), 1503, 1365, 1243, 1165, 1069, 957, 907, 735, 698 and 608.

2-Benzyloxy-ethylamine (8)—Trifluoroacetic acid (60 mL) was added drop-wise to a solution of the carbamate **5** (18 g, 72 mmol) in CH_2Cl_2 (150 mL) at 0 °C over a period of 1 h. The reaction mixture was then stirred at room temperature for 18 hours. The solvents were removed under reduced pressure and the residue was divided between EtOAc (150 mL) and 5% aq. Na_2CO_3 solution (150 mL). The organic layer was washed with brine, dried (Na_2SO_4) and the solvents removed under vacuum. The residue was purified by column chromatography over silica gel eluting with chloroform to afford the title compound as a pale yellow oil (10.3 g, 95%). R_f = 0.06 ($CHCl_3$, SiO_2); ^{1}H NMR (270 MHz, $CDCl_3$) δ = 7.31 (5H, m, Ar), 4.48 (2H, s, OCH_2Ar), 3.47 (2H, t, $^3J_{H\text{-}H}$ = 5 Hz, NCH_2CH_2O), 2.85 (2H, t, $^3J_{H\text{-}H}$ = 5 Hz, NCH_2CH_2O), 1.29 (2H, s br, NH_2); ^{13}C NMR (67.5 MHz, $CDCl_3$) δ = 138.4 (Ar), 128.5 (Ar), 127.7 (Ar), 73.2 (OCH_2Ar), 72.7 (CH_2CH_2O), 42.1 (NHCH_2CH_2); *m/z* (ESI+) 152 (100%, $[M+H]^+$); ν_{max} / cm^{-1} (thin film): 3029 (NH), 2924, 2854, 1652, 1454, 1355, 1205, 1101, 739, 698, 546.

1,3-Bisbenzyloxy-2-aminopropane(9)—The title compound was prepared according to the procedure used for compound **8** using the carbamate **6** (20.0 g, 56.0 mmol) and triflouroacetic acid (60 mL). The title compound was obtained as a pale yellow oil (15.0 g, 98%). R_f = 0.07 ($CHCl_3$, SiO_2); ^{1}H NMR (270 MHz, $CDCl_3$) δ = 7.33 (5H, m, Ar), 4.52 (4H, s, OCH_2Ar), 3.48 (4H, m, CHCH_2O), 3.22 (1H, m, NHCH), 1.72 (2H, s, NH_2); ^{13}C NMR (67.5 MHz, $CDCl_3$) δ = 138.4 (Ar), 128.5 (Ar), 127.8 (Ar), 73.4 (OCH_2Ar), 72.8 (CHCH_2O), 51.2 (NHCH); *m/z* (ESI+) 273 (100%, $[M+H]^+$), 294 (80%, $[M+Na]^+$); ν_{max} / cm^{-1} (thin film): 3067, 2859, 1681, 1491, 1452, 1362, 1202, 1094, 1027, 800, 737, 698 and 607.

Trisbenzyloxymethyl aminomethane (10)—The title compound was prepared according to the procedure used for compound **8** using the carbamate **7** (25.0 g, 49 mmol) and triflouroacetic acid (100 mL). The title compound was ontained as a pale yellow oil (18.5 g, 95%). R_f = 0.05 ($CHCl_3$, SiO_2); ^{1}H NMR (270 MHz, $CDCl_3$) δ = 7.36 (5H, m, Ar), 4.54 (6H,

s, OC$\underline{H}_2$Ar), 3.51 (6H, s, CC$\underline{H}_2$O), 1.70 (2H, s, N$\underline{H}_2$); ^{13}C NMR (67.5 MHz, $CDCl_3$) δ = 138.7 (Ar), 128.4 (Ar), 127.6 (Ar), 73.5 (O$\underline{C}H_2$Ar), 72.7 (C$\underline{C}H_2$O), 58.3 (NH$\underline{C}CH_2$O); *m/z* (ESI+) 392 (75%, $[M+H]^+$), 414 (100%, $[M+Na]^+$); ν_{max} / cm^{-1} (thin film): 3280 (NH), 3031, 2864, 1691, 1453, 1367, 1202, 1090, 1027, 909, 799, 736, 698 and 606.

2-Benzyloxyethyl-2-bromoacetamide (11)—Potassium carbonate (11.6 g, 84 mmol) was added to a solution of the amine **8** (9.0 g, 60 mmol) in dichloromethane (250 mL) and the suspension was cooled to 0 °C in an ice bath. Bromoacetyl bromide (17.0 g, 84 mmol) was added drop-wise to the vigorously stirred reaction mixture over a period of 1 hour. The reaction mixture was then allowed to warm to room temperature and stirred for a further 18 hours. Water (100 mL) was then added and the two layers separated. The organic layer was dried (Na_2SO_4) and the solvents removed under reduced pressure. The residue was then purified by column chromatography over silica gel eluting with chloroform to afford title compound as a pale yellow oil (14.6, 90%). R_f = 0.18 ($CHCl_3$, SiO_2); ^{1}H NMR (270 MHz, $CDCl_3$) δ = 7.33 (5H, m, Ar), 6.94 (1H, s br, N$\underline{H}$), 4.50 (2H, s, OC$\underline{H}_2$Ar), 3.82 (2H, s, BrC$\underline{H}_2$CO), 3.55 (2H, t, $^3J_{H\text{-}H}$ = 5 Hz, $CH_2C\underline{H}_2O$), 3.49 (2H, t, $^3J_{H\text{-}H}$ = 5 Hz, NC$\underline{H}_2CH_2$); ^{13}C NMR (67.5 MHz, $CDCl_3$) δ = 165.7 (C=O), 137.9 (Ar), 128.6 (Ar), 127.9 (Ar), 73.2 (O$\underline{C}H_2$Ar), 68.4 ($CH_2\underline{C}H_2O$), 40.1 (N$\underline{C}H_2CH_2$), 29.2 (Br$\underline{C}H_2$CO); *m/z* (ESI+) 272 (100%, $[M+H]^+$), 294 (20%, $[M+Na]^+$) appropriate isotope patterns were observed, ν_{max} / cm^{-1} (thin film): 3291 (NH), 3064, 2865, 1717, 1654 (C=O), 1540, 1453, 1355, 1274, 1211, 1100, 1027, 740, 698.

(2-Propyl-1,3-bisbenzyloxyl)-bromoacetamide (12)—The title compound was prepared according to the procedure used for compound **11** using the amine **9** (14.0 g, 52.0 mmol), potassium carbonate (10.0 g, 72.0 mmol) and bromoacetyl bromide (14.6 g, 72.0 mmol). The title compound was obtained by column chromatography over silica gel eluting with 5% ethyl acetate in chloroform as a colourless solid (18.4 g, 90 %). R_f = 0.42 (5% EtOAc in $CHCl_3$, SiO_2); ^{1}H NMR (270 MHz, $CDCl_3$) δ = 7.33 (5H, m, Ar), 6.89 (1H, d, $^3J_{H\text{-}H}$ = 8 Hz, CON$\underline{H}$), 4.53 (4H, s, OC$\underline{H}_2$Ar), 4.25 (1H, ddd, $^3J_{H\text{-}H}$ = 5 Hz, $^3J_{H\text{-}H}$ = 5 Hz, $^3J_{H\text{-}H}$ = 8 Hz, NHC$\underline{H}$(CH_2)$_2$), 3.84 (2H, s, BrC$\underline{H}_2$CO), 3.66 (2H, d, $^3J_{H\text{-}H}$ = 5 Hz, CHC$\underline{H}_2$O), 3.58 (2H, d, $^3J_{H\text{-}H}$ = 5 Hz, CH(C$\underline{H}_2$O)$_2$); ^{13}C NMR (67.5 MHz, $CDCl_3$) δ = 165.2 (C=O), 138.0 (Ar), 128.5 (Ar), 127.8 (Ar), 73.3 (O$\underline{C}H_2$Ar), 68.2 (CH$\underline{C}H_2$O), 49.4 (NH$\underline{C}$HCH$_2$), 29.3 (Br$\underline{C}H_2$CO); *m/z* (ESI+) 492 (90%, $[M+H]^+$), 414 (100%, $[M+Na]^+$), 432 (50%, $[M+K]^+$) appropriate isotope patterns were observed; ν_{max} / cm^{-1} (thin film): 3301 (NH), 3060, 2858, 1719, 1649 (C=O), 1547, 1453, 1366, 1256, 1123, 1026, 736 and 695.

Bromoacetamido *N*-(tris benzyloxymethyl)-methane (13)—The title compound was prepared according to the procedure used for compound **11** using the amine **10** (15.0 g, 38.0 mmol), potassium carbonate (7.5 g, 54.0 mmol) and bromoacetyl bromide (10.8 g, 54.0 mmol). The title compound was obtained by column chromatography over silica gel eluting with 5% ethyl acetate in chloroform as a pale yellow oil (16.7 g, 85%). R_f = 0.2 (5% EtOAc in $CHCl_3$, SiO_2); ^{1}H NMR (270 MHz, $CDCl_3$) δ = 7.35 (5H, m, Ar), 6.92 (1H, s, N$\underline{H}$), 4.57 (6H, s, OC$\underline{H}_2$Ar), 3.94 (6H, s, CC$\underline{H}_2$O), 3.81 (2H, s, BrC$\underline{H}_2$CO); ^{13}C NMR (67.5 MHz, $CDCl_3$) δ = 165.4 (C=O), 138.3 (Ar), 128.5 (Ar), 127.7 (Ar), 73.6 (O$\underline{C}H_2$Ar), 68.8 (C$\underline{C}H_2$O), 60.6 ($\underline{C}CH_2$O), 29.9 (Br$\underline{C}H_2$CO); *m/z* (ESI+) 512 (40%, $[M+H]^+$), 534 (60%, $[M+Na]^+$) appropriate isotope patterns were observed; ν_{max} / cm^{-1} (thin film): 3380 (NH), 3031, 2863, 1726, 1657 (C=O), 1530, 1453, 1365, 1273, 1207, 1098, 1026, 738, 698 and 607.

(2-Benzyloxy ethyl)-1,4,7,10-tetraazacyclododecane-1,4,7,10-tetraacetamide (14)—The bromoacetamide **11** (7.89g, 29.0 mmol) and cyclen (1.0 g, 58 mmol) were dissolved in anhydrous acetonitrile (200 mL) and potassium carbonate (9.62 g, 70.0 mmol) added. The resulting suspension was heated under reflux, with stirring, for 6 days. After cooling to room temperature the solvents were removed under reduced pressure and the residue taken up into

H_2O (100 mL) and CH_2Cl_2 (100 mL). The organic layer was separated and the aqueous layer extracted with CH_2Cl_2 (3 × 15 mL). The combined extracts were dried (Na_2SO_4) and the solvents were removed under reduced pressure. The residue was purified by column chromatography over silica gel eluting with 5% MeOH in CH_2Cl_2 to afford the title compound as a yellowish solid (3.4 g, 63%). R_f = 0.08 (5% MeOH in CH_2Cl_2, SiO_2); ^{1}H NMR (270 MHz, $CDCl_3$) δ = 7.49 (4H, t, $^3J_{H-H}$ = 8 Hz, CONHCH$_2$), 7.27 (20H, m, Ar), 4.44 (8H, s, CH$_2$Ar), 3.50 (8H, t, $^3J_{H-H}$ = 5 Hz, CH$_2$CH$_2$O), 3.42 (8H, dt, $^3J_{H-H}$ = 8 Hz, $^3J_{H-H}$ = 5 Hz, NHCH$_2$CH$_2$), 2.87 (8H, s, NCH$_2$CO), 2.47 (16H, s, ring NCH$_2$); ^{13}C NMR (67.5 MHz, $CDCl_3$) δ = 170.9 (C=O), 138.0 (Ar), 128.5 (Ar), 128.0 (Ar), 73.2 (OCH$_2$Ph), 69.0 (CH$_2$CH$_2$O), 59.4 (NCH$_2$CO), 54.0 (ring NCH$_2$), 39.2 (NHCH$_2$CH$_2$); *m/z* (ESI+) 938 (50%, $[M+H]^+$), 960 (100%, $[M+Na]^+$); ν_{max} / cm^{-1} (thin film): 3201 (NH), 3062, 2966, 2827, 1666 (C=O), 1550, 1453, 1366, 1309, 1237, 1102, 1002, 816, 741, 699 and 601; Anal found: C = 64.2%, H = 7.5%, N = 11.4%, $C_{52}H_{72}N_8O_8 \cdot 2H_2O$ requires C = 64.2%, H = 7.8%, N = 11.5%.

(2-propyl-1,3-bisbenzyloxy)-1,4,7,10-tetraazacyclododecane-1,4,7,10-tetraacetamide (15)—The title compound was prepared according to the procedure used for compound **11** using the bromoacetamide **12** (11.4 g, 29.0 mmol), cyclen (1.0 g, 5.8 mmol) and potassium carbonate (9.6 g, 70.0 mmol). The title compound was obtained as a yellow semi-solid (4.4 g, 54%). R_f = 0.07 (5% MeOH in CH_2Cl_2, SiO_2); ^{1}H NMR (270 MHz, $CDCl_3$) δ = 7.30 (40H, br, Ar), 6.88 (4H, d, $^3J_{H-H}$ = 9 Hz, CONH), 4.38 (16H, s, OCH$_2$Ar), 4.28 (4H, m, NHCHCH$_2$), 3.53 (16H, m, CHCH$_2$O), 2.83 (8H, s, NCH$_2$CO), 2.44 (16H, s, ring NCH$_2$); ^{13}C NMR (67.5 MHz, $CDCl_3$) δ = 171.0 (C=O), 138.34 (Ar) 128.4(Ar), 127.9 (Ar), 73.2 (OCH$_2$Ar), 69.4 (CHCH$_2$O), 56.7 (NHCHCH$_2$), 50.3 (ring NCH$_2$), 48.6 (NCH$_2$CO); *m/z* (ESI+) 1418 (70%, $[M+H]^+$), 1440 (100%, $[M+Na]^+$), 1458 (20%, $[M+K]^+$); ν_{max} / cm^{-1} (thin film): 3156, 2968, 1670 (C=O), 1539, 1452, 1364, 1310, 1206, 1103, 1027, 908, 816, 738, 698 and 607; . Anal. found: C = 68.4%, H = 7.3%, N = 7.5%, $C_{84}H_{104}N_8O_{12} \cdot 3H_2O$ requires C = 68.6%, H = 7.5%, N = 7.6%.

(1,1-bisbenzyloxymethyl-2-hydroxyethane)-1,4,7,10-tetraazacyclododecane-1,4,7,10-tetra acetamide (16)—The bromoacetamide **13** (14.9 g, 29.0 mmol) and cyclen (1.0 g, 5.8 mmol) were dissolved in anhydrous acetonitrile (250 mL) and anhydrous diisopropylethylamine (20.0 mL, 115.0 mmol) added. The resulting reaction mixture was heated under reflux, with stirring under an argon atmosphere, for 6 days. The solvents were removed under reduced pressure and the residue taken up in water (100 mL) and CH_2Cl_2 (100 mL). The organic layer was separated and the aqueous layer was extracted with CH_2Cl_2 (3 × 15 mL). The combined organics were dried (Na_2SO_4) and the solvents were removed under reduced pressure. The residue was purified by column chromatography over silica gel eluting with CH_2Cl_2 followed by 5% MeOH in CH_2Cl_2 to afford the title compound as pale yellow semi-solid (4.62 g, 42%). R_f = 0.05 (5% MeOH in CH_2Cl_2, SiO_2); ^{1}H NMR (270 MHz, $CDCl_3$) δ = 7.24 (60H, m, Ar), 7.04 (4H, s, br, NH), 4.45 (24H, s, OCH$_2$Ar), 3.86 (24H, s, CCH$_2$O), 2.67 (8H, s, NCH$_2$CO), 2.34 (16H, s, ring NCH$_2$); ^{13}C NMR (67.5 MHz, $CDCl_3$) δ = 170.7 (C=O), 138.4 (Ar), 128.5 (Ar), 127.8 (Ar), 73.4 (OCH$_2$Ar), 69.1 (CCH$_2$O), 60.5 (NCH$_2$CO), 59.7 (NHCCH$_2$O), 52.3 (ring NCH$_2$); *m/z* (ESI+) 1899 (30%, $[M+H]^+$), 1821 (100%, $[M+Na]^+$), 1935 (30%, $[M+K]^+$); ν_{max} / cm^{-1} (thin film): 3412 (NH), 3109, 2948, 2810, 1952, 1876, 1685 (C=O)), 1560, 1516, 1464, 1363, 1312, 1102, 1027, 901, 812, 738, 697 and 605; Anal. found: C = 69.7%, H = 7.1%, N = 5.6%, $C_{116}H_{136}N8O_{16} \cdot 5H_2O$ requires C = 70.0%, H = 7.4%, N = 5.6%.

(2-hydroxy ethyl)-1,4,7,10-tetraazacyclododecane-1,4,7,10-tetra acetamide (L^4)—The tetraether **14** (3.24 g, 35 mmol) was dissolved in anhydrous MeOH (35 mL) and glycial acetic acid (10 mL), after degassing with argon, dried Pearlman catalyst ($Pd(OH)_2$/C, 2.5 g) was added. The reaction was placed on a Parr hydrogenation apparatus and shaken under a

hydrogen pressure of 65 psi for 2 days. To the slurry was added water (10 mL) and the mixture stirred for 5 min. The catalyst was then removed by filteration and the solvents removed under reduced pressure. The residue was taken up in water (20 mL) and loaded on to a column of Amberlite IRA 400 ion exchange resin (OH- form). The column was eluted with distilled water and lypholization afforded the title compound as a pale yellow solid (1.7 g, 85%). ^{1}H NMR (270 MHz, D_2O) δ = 3.63 (8H, t, $^3J_{H\text{-}H}$ = 5 Hz, $CH_2C\underline{H}_2OH$), 3.33 (8H, t, $^3J_{H\text{-}H}$ = 5 Hz, $NHC\underline{H}_2CH_2$), 3.14 (8H, s, $NC\underline{H}_2CO$), 2.67 (16H, s, ring $NC\underline{H}_2$); ^{13}C NMR (67.5 MHz, D_2O) δ = 174.3 ($\underline{C}$=O), 60.1 ($CH_2\underline{C}H_2OH$), 58.5 ($N\underline{C}H_2CO$), 52.4 (ring $N\underline{C}H_2$), 41.5 ($NH\underline{C}H_2CH_2$); *m/z* (ESI+) 577 (100%, $[M+H]^+$), 599 (60%, $[M+Na]^+$); ν_{max} / cm^{-1} (thin film): 3460 (NH), 2942, 2827, 1653 (C=O), 1559, 1455, 1369, 1241, 1065, 1003, 603; Anal. found: C = 44.6%, H = 8.2%, N = 16.7%, $C_{24}H_{48}N_8O_8{\cdot}4H_2O$ requires C = 44.5%, H = 8.7%, N = 17.2%.

(2-propyl-1,3-bishydroxy)-1,4,7,10-tetraazacyclododecane-1,4,7,10-tetraacetamide (L^8)—The title compound was prepared according to the procedure used for compound **L^4** using the tetraether **15** (3.8 g, 2.7 mmol) and Pearlman catalyst ($Pd(OH)_2$/C, 2.5 g). The title compound was obtained as a pale yellow solid (1.6 g, 88%). ^{1}H NMR (270 MHz, D_2O) δ = 4.03 (4H, m, $C\underline{H}CH_2OH$), 3.71 (16H, m, $CHC\underline{H}_2OH$), 3.23 (8H, s, $NC\underline{H}_2CO$), 2.75 (16H, s, ring $NC\underline{H}_2$); ^{13}C NMR (67.5 MHz, D_2O) δ = 174.1 ($\underline{C}$=O), 60.7 ($CH_2\underline{C}H_2OH$), 58.7 ($N\underline{C}H_2CO$), 52.8 ($NH\underline{C}HCH_2$), 52.1 (ring $N\underline{C}H_2$); *m/z* (ESI+) 698 (60%, $[M+H]^+$), 720 (100%, $[M+Na]^+$); ν_{max} / cm^{-1} (thin film): 3382 (NH), 2946, 2830, 1658 (C=O), 1558, 1457, 1369, 1278, 1049, 1008 and 602; Anal. found: C = 45.3%, H =8.3%, N = 14.6%, $C_{28}H_{56}N_8O_{12}{\cdot}2.85H_2O$ requires C = 45.0%, H = 8.3%, N = 14.9%.

(1,1-bishydroxymethyl-2-hydroxyethane)-1,4,7,10-tetraazacyclododecane-1,4,7,10-tetra acetamide (L^{12})—The title compound was prepared according to the procedure used for compound **L^4** using the tetra ether **16** (4.0 g, 2.1 mmol), Pearlman catalyst ($Pd(OH)_2$/C, 2.5 g) and 70 psi of hydrogen. The title compound was obtained as a pale yellow solid (0.95 g, 55%). ^{1}H NMR (270 MHz, D_2O) δ = 3.77 (24H, s, $CC\underline{H}_2OH$), 3.54 (8H, s, $NC\underline{H}_2CO$), 2.97 (16H, s, ring $NC\underline{H}_2$); ^{13}C NMR (67.5 MHz, D_2O) δ = 173.4 ($\underline{C}$=O), 60.8 ($C\underline{C}H_2OH$), 58.5 ($N\underline{C}H_2CO$), 51.3 ($NH\underline{C}CH_2$), 50.8 (ring $N\underline{C}H_2$); *m/z* (ESI+) 818 (40%, $[M+H]^+$), 840 (100%, $[M+Na]^+$); ν_{max} / cm^{-1} (thin film): 3352 (NH), 2945, 2845, 1683 (C=O), 1559, 1458, 1394, 1297, 1052, 947 and 644; Anal. found C = 43.3%, H = 8.1%, N = 12.1%, $C_{32}H_{64}N_8O_{16}{\cdot}4.5H_2O$ requires C = 42.8%, H = 8.2%, N = 12.4%.

Stock solutions and complex preparation

Stock solutions of lanthanide chloride salts were prepared from the commercially available chloride salts. Stock solutions were prepared at concentrations between 0.02 and 0.70 M (solution pH ranging from 3 – 5) and the concentrations determined by complexometric titration with standardized Na_2H_2EDTA solution and xylenol orange indicator. Na_2H_2EDTA solution was purchased from Alfa-Aesar and its concentration was determined by pH potentiometric titration with standardized KOH solution. Stock solutions of ligands L^4, L^8 and L^{12} at concentrations between 0.02 and 0.04 M) were prepared in deionized water. The pH of these solutions was maintained in the range 3 – 4 with HCl. The concentrations of the ligand stock solutions were determined by pH-potentiometry from titration data obtained in the absence and in the presence of a 50 to 100 fold excess of $CaCl_2$.

General procedures for the preparation of the Ln^{3+} complexes

The lanthanide complexes of L^4, L^8 and L^{12} were prepared as their triflate salts by mixing equimolar quantities of the appropriate lanthanide triflate and ligand in a 1:1 acetonitrile/ methanol solution and heating at 50 °C for 3 days. The solvents were then removed under

reduced pressure, the residue taken up into water and freeze dried to afford the complex which was used without further purification.

Chloride salts of L^4, L^8 and L^{12} lanthanide complexes were prepared from an appropriate standardized lanthanide chloride solution and an equimolar quantity of ligand in aqueous solution. The solution pH was adjusted to 5.5 using 1 M NaOH and 1 M HCl as necessary and the reaction mixture stirred at room temperature. The reaction pH was maintained in the range 5.0 – 5.5 by addition of 1 M NaOH solution. Reaction progress was monitored with xylenol orange indicator (0.15 M AcOH/AcONa buffer, pH 5.5). When the indicator indiacted that no free lanthanide remained the pH was raised to 7 (1M NaOH), filtered and freeze-dried to afford the complex which was used without further purification.

Potentiometric measurements

The pH-potentimetric titrations were carried out with a Thermo Orion expandable ion analyzer EA940 pH meter using Thermo Orion semi-micro combination electrode 8103BN in vessels thermostated at 25.0°C. Metrohm, DOSIMATE 665 autoburette with a 5 mL capacity was used for base additions. 1.0 M KCl was used to maintain the ionic strength. All equilibrium measurements (direct titrations) were carried out in 10.00 mL sample volumes with magnetic stirring. During the titrations argon gas was passed over the top of the samples in order to ensure CO_2-free conditions in the potentiometric cell. Electrode calibration was performed using standard buffers purchased from VWR (pH = 4.005 and pH = 9.180). The titrant, carbonate-free KOH solution, was standardized with 0.05 M KH-phthalate solution by pH-potentiometric titration. A standard solution of hydrochloric acid was prepared by dilution of conc. HCl with doubly distilled water and its concentration determined by pH-potentiometric titration with the standardized KOH solution. The $[H^+]$ was determined using a published method [10]. The pK_w of water was calculated from these titration data and found to be 13.721.

The protonation constants ($\log K_i^H$) and stability constant values were determined by using the PSEQUAD computer program [11].

Protonation and thermodynamic stability constant determination

The protonation constants of the ligands L^4, L^8 and L^{12} were determined by titrating solutions of the ligands at 2.0 – 4.0 mM with a standardized KOH solution (0.171 M) over the pH range 1.8 – 12.0 (160–210 data points). The protonation constants of the ligand ($\log K_i^H$) are defined according to equation (1), where i = 1, 2, 3…. and $[H_{i\text{-}1}L]$ and $[H^+]$ are the equilibrium concentrations of the ligand (i = 1), protonated forms of the ligand (i = 2 or 3) and hydrogen ion respectively.

$$K_i^H = \frac{[H_i L]}{[H_{i-1} L][H^+]} \tag{1}$$

To determine the thermodynamic stability constants of divalent metal ions titrations were carried out using 1:1 and 1:2 ligand / metal ratios with the concentration of the ligand maintained at about 2.0 mM. The combined titration data were fitted simultaneously and the thermodynamic stability constants (K_{ML}) were evaluated and reported based on equation (2).

$$K_{ML} = \frac{[ML]}{[M][L]} \tag{2}$$

Because the complexes of lanthanide ions with DOTA-tetraamide ligands form very slowly the thermodynamic stability constants of L^4, L^8 and L^{12} with lanthanide ions were determined

using “out-of-cell” experiments.[5,11] Typically, 25.0 mL of an equimolar solution of $LnCl_3$ and ligand, concentration ~ 2.0 mM, was prepared and divided in to 16 individual solutions (1.5 mL each). The pH of each sample was then adjusted to a different pH value using HCl or KOH solution such that the samples covered the pH range of 2.5 – 5.0. The samples were properly sealed and placed in a 40 °C incubator for 35 days followed by an additional 35 days at room temperature to re-equilibrate the mixture to room temperature. The pH of each individual sample was then measured. The proton concentration was calculated from the measured pH values using a correction term determined according to Irving *et al* [10] by titration of 14 mM strong acid (HCl) with 0.1713 M KOH as a difference between the measured and calculated pH values. Such titration was performed before and after the pH measurement in the batch samples and the average of these two measurements was used as a correction term.

Kinetic measurements

The formation rates of CeL^4 and CeL^8 were measured by spectrophotometry using a Cary 300 Bio UV-Vis spectrophotometer equipped with thermostated cell holder and semi-micro quartz cells (Starna, optical path length 1.0 cm). Solutions containing 1.0 mM ligand and a 10 – 50-fold excess of $CeCl_3$ were studied and complex formation was monitored at 324 nm and 25 ° C. The ionic strength was maintained at 1.0 M with KCl and pH controlled with 0.05 M non-coordinating buffers: *N*-methylpiperazine (NMP, log K_1^H = 4.83) and piperazine (PIP, log K_1^H = 6.04 at I = 1.0 M and 25 °C) [12]. Absorbance was data recorded as a function of time and fitted to equation (3) to evaluate the first-order rate constants, where A_0, A_t, and A_e are the absorbance values measured at time = 0, time = t and at equilibrium, respectively.

$$A_t = A_e + (A_0 - A_e) \times e^{(-k_{obs} \times t)} \quad (3)$$

All the dissociation kinetics were performed on 2.0 mM solutions of CeL complex in 0.5 – 3.0 M HCl at 25 °C. The total ionic strength ([KCl] + [HCl]) was 3.0 M. The decrease Ce^{3+} in absorbance was measured as a function of time at 324 nm.

Radiochemistry

Lutetium-177 chloride in 0.05 N HCl was purchased from the University of Missouri Research Reactor (MURR, MO) at a typical specific activity of 24.48 Ci/mg. All reaction vials were acid washed with 10–20% nitric acid overnight. Milli-Q water (18 MΩ-cm) was obtained from a Millipore Gradient Milli-Q water system (Billerica, MA) and used for all radiochemistry procedures and biological evaluations. Under no-carrier added (n.c.a) condition, all the ligands were labelled with ^{177}Lu by adding 1 μL of $^{177}LuCl_3$ solution (~ 400 μCi) to 100 μL of 0.4 M ammonium acetate (pH = 7.0) containing a ligand in the concentration of 5 mM. The resulted solutions were incubated at 60 °C for 2 h in an Eppendorf thermomixer at 1,000 rpm. The carrier-added (c.a.) [^{177}Lu]Lu(III) complexes were prepared under similar conditions by adding a $LuCl_3$ solution pre-mixed with ^{177}Lu to a ligand solution with the molar ratio of ligand/Lu(III) maintained at 1.2 : 1. The radiochemical yields and purity were determined by Radio-TLC analysis.

Determination of Partition Coefficients

The partition coefficients (*log P*) of the ^{177}Lu-labeled complexes were determined by adding 10 μL of each ^{177}Lu-labeled complex to a biphasic solution containing 500 μL of *n*-octanol (water saturated) and 500 μL of Mini-Q water (n = 5). The resulting solutions were then shaken for 3 h at room temperature. From each of the five samples an aliquot of 100 μL was removed from each phase and counted separately. The partition coefficient was calculated as an average logarithm value (log P) of the ratio of the counts in the octanol fraction to the counts in the water fraction from the five samples.

Serum Stability

The in vitro stability in serum was evaluated by incubating 10 μL of each ^{177}Lu-labeled complex with 100 μL of rat serum at 37 °C. At specific time points, an aliquot of the solution was taken out and analyzed by radio-TLC.

Pharmacokinetic and Biodistribution Studies

All animal studies were performed in compliance with guidelines set by the UT Southwestern Institutional Animal Care and Use Committee. The injection doses were prepared by diluting each ^{177}Lu-labeled complex with 10 mM PBS buffer. Normal 4 – 5 week old male healthy balb/c mice (Harlan, IN) were anesthetized with isoflurane and then injected with 100 μL of each ^{177}Lu-labeled complex (*ca*. 5 μCi/mouse) via the tail vein. The animals were anesthetized again prior to sacrifice at 30 min, 1 h, 4 h, 24 h, and 48 h post-injection (p.i.) (n = 4 at each time point). Organs of interest (blood, heart, lung, liver, spleen, kidney, fat, muscle, intestine, stomach, and bone) were removed, weighed, and counted. Standards were prepared and counted along with the samples to calculate the percent injected dose per gram tissue (%ID/g) and percent injected dose per organ (%ID/organ). The animals of the last time point groups were housed in metabolic cages (4 mice per cage) to collect urine and feces at 1 h, 4 h, 24 h and 48 h post-injection. For the evaluation of pharmacokinetic parameters, 5 – 10 μL of blood was collected from the retroorbital sinus of the animals at 2, 5, 10, 15, 30, 60 and 240 min.

The biodistribution of carrier-added (c.a.) complexes was performed in the same way as above. The injection doses were prepared by reconstituting each [^{177}Lu]Lu complex with 10 mM PBS buffer to make a final volume of 100 μL for each dose containing 2 μmoles of the complex. In light of the acute toxicity that could be caused by the high injected dose, all animals received the c.a. complexes were closely watched regarding their appearance, behavior, and weight loss after the intravenous injection. The animals injected with [^{177}Lu]Lu complexes of L^1, L^4, and L^8 immediately became panic, struggling, and dead within 5 min p.i. (n = 4). The acute toxicity experiments were repeated for the three complexes and the results were the same. No apparent toxic effects were observed on the animals received [^{177}Lu]LuL^{12}, which were sacrificed at 4 h, 24 h, and 48 h p.i. (n = 4 at each time point) for biodistribution studies as detailed above. The unpaired *t*-test on the biodistribution data was performed using Prism, v. 4.00 (Graphpad, San Diego, CA USA).

Results and Discussion

Ligand Synthesis

For this study, 1,4,7,10-tetraazacyclododecane (cyclen) serves as the central building block for L^4 , L^8, and L^{12} (Chart 2). The pendant ligating amides were prepared *via* selective protection (-OH → -OR) methods to generate the appropriate α-bromo electrophiles for subsequent *N*-alkylation of cyclen with regeneration of the polyol functionality in the final step. A common synthetic strategy was adopted for the synthesis of L^4, L^8 and L^{12} ligands. A Boc protected amino alcohol was chosen as the starting point in each synthesis. In the case of L^4 and L^8, suitable Boc protected starting materials were commercially available (Scheme 1) while in the case of L^{12}, the amine had to be Boc protected by reaction with di-*tert*-butyl carbonate. The hydroxyl groups could then be protected as benzyl ethers using benzyl bromide and potassium hydroxide as base. In the case of the synthesis of ether **3**, only one benzyl group had to be introduced because one hydroxyl group was already protected.

Deprotection of the amino groups was performed using triflouroacetic acid (TFA) followed by base extraction to afford the free base. The bromoacetamides **11, 12** and **13** were synthesized by reaction of the free amines **8, 9** and **10** with bromoacetyl bromide, with potassium carbonate as base. These bromoacetamides were then used to alkylate cyclen using five equivalents of

alkylating agent, potassium carbonate as base (Hünig's base was used in the case of L^{12}) and acetonitrile as solvent. The protected ligands **14, 15** and **16** were obtained following column chromatography over silica gel. The use of Hünig's base in the case of **16** promoted better yields and avoided the sometimes problematic potassium complex formation with the ligand. Deprotection of the hydoxyl groups was found to be problematic because the benzyl ethers proved resistant to standard procedures (H_2 and 10% Pd on C). After numerous procedures were attempted, benzyl deprotection was finally accomplished by means of hydrogenolysis in presence of dry Pearlman catalyst ($Pd(OH)_2$ on carbon) in 22% v/v acetic acid in methanol. Exhaustive deprotection of the ethers **14, 15** and **16** afforded the target ligands L^4, L^8 and L^{12} in 85%, 88% and 55% overall yield, respectively. The europium and cerium complexes of ligands L^4, L^8 and L^{12} were prepared using the appropriate lanthanide triflate in an acetonitrile/methanol mixture or from the chloride salts in water.

Complex kinetics and stability

Two factors describe the stability of a complex, its thermodynamic stability, defined by equation 2, and its kinetic inertness - its resistance to dissociation. The thermodynamic stability constant ($log\ K_{ML}$) of a complexes can be determined by pH-potentiometry. The protonation constants ($log\ K_i^H$) of ligands L^4 and L^8 were determined by potentiometric titration in a 1.0 M KCl ionic background. Although the K^+ ion is known to form weak complexes with DOTA-tetraamide ligands this choice of ionic background allows our data to be compared with that reported previously for similar systems [5–7]. Both L^4 and L^8 were found to have two protonation constants (Table 1) and by comparison with related systems these can be assigned to the protonation of opposing nitrogen atoms of the macrocyclic ring [5–7]. In each case the absolute value of the first protonation constant is slightly lower, by about half a log unit, than those observed for other tetraamides. In contrast the absolute value of the second protonation constant is in the range, or slightly higher, than those of other tetraamides. Thus the total basicity, or the sum of the protonation constants, of these ligands is approximately the same as that observed for other simple DOTA-tetraamide derivatives suggesting that L^4 and L^8 should form complexes of comparable stability.

The complexes of L^4 and L^8 with the endogenous divalent metal ions Mg^{2+}, Ca^{2+}, Cu^{2+} and Zn^{2+} form quickly enough that their thermodynamic stability constants could be determined by direct potentiometric titration of the ligand in the presence of the metal ion. The thermodynamic stability constants determined for these complexes are shown in Table 1. It is worthy of note that the stability of the Mg^{2+}, Ca^{2+} and Cu^{2+} complexes of L^4 and L^8 are comparable to those of other DOTA-tetraamide complexes. However, the Zn^{2+} complexes appear to be slightly, if significantly, more stable; the $log\ K_{ZnL}$ of L^8 is about 0.5 – 0.6 log units higher than simple DOTA-tetraamide complexes whereas the $log\ K_{ZnL}$ of L^4 is about 1.3 log units higher.

Determining the stability constants of complexes with L^{12} proved to be a somewhat intractable problem. Rather surprisingly, a potentiometric titration of the L^{12} was consistent with six protonation constants in the range 2 – 12. We have been unable to find literature examples of either amide or hydroxyl protons that have protonation constants in this range and yet, these are the only plausible candidates to which the four unexpected protonation constants can be assigned. By performing the potentiometric titration in the presence of a metal ion that rapidly forms complexes it is normally possible to identify protonation constants of groups involved in complex formation. The Ca^{2+} ion is ideal for this purpose; its coordination chemistry is comparable to that of the Ln^{3+} ions although it forms complexes much more rapidly and it does not form hydroxo complexes in the required pH range ($\log \beta_{-11} = -12.8$) [13]. Titrating L^{12} in the presence of 1 and 2 equivalents of $CaCl_2$ afforded a curve that was identical to that obtained in the absence of Ca^{2+}. Only when a considerable excess of $CaCl_2$ was employed

could an inflection point due neutralization of protons liberated by complex formation be observed. A second inflection point corresponding to the neutralisation of protons not displaced by formation for the complex is also observed (supplementary information S1). This behaviour may be the result of slower or weaker than usual complex formation between Ca^{2+} and L^{12}. The closeness of the values of the protonation constants observed for L^{12} coupled with uncertainty in the behaviour of this system in the presence of Ca^{2+} means that potentiometry could not be used to establish definitive protonation constants for those groups involved in complex formation. A ^{1}H NMR titration performed on this system afforded no additional evidence to help clarify this problem. In the absence of reliable protonation constant data for L^{12} the thermodynamic stability constants of complexes of this ligand were not determined in this work, an alternative technique that will afford this information is being sought.

The formation of lanthanide complexes with DOTA-tetraamide ligands is much too slow to be measured by direct potentiometric titration. For this reason an “out-of-cell” approach was used to measure these stability data [17]. The *log* K_{LnL} values determined for both LnL^4 and LnL^8 compelxes follow a similar trend across the lanthanide series, rising across the early lanthanides before peaking around the middle of the series and decreasing slightly at the later lanthanide ions (Table 2). The increase in stability across the early lanthanides is also observed for other DOTA-tetraamide systems. However, the decrease in stability over the later lanthanides is more marked than that observed for any of the other DOTA-tetraamides in Table 2, indeed some of these other complexes continue to increase in stability across the late lanthanides. The stability constants of LnL^4 and LnL^8 complexes are slightly lower than those determined for most other DOTA-tetraamide systems, a reflection of the lower first protonation constants observed for these ligands.

For a lanthanide complex to be considered safe for use *in vivo*, it is imperative that it be excreted from the body intact prior to any metal ion release from the ligand. Thus, for *in vivo* applications, kinetic inertness is a more important factor in determining safety than the thermodynamic stability constant of the complex. The rates of dissociation of DOTA-tetraamide complexes are extremely slow [5], therefore in order to measure such rates a large excess of acid must be used in order to accelerate the process. The rate of the acid catalysed dissociation of Ce^{3+} complexes is readily measured by UV absorbance, following the coordination environmentally sensitive $4f^1 \rightarrow 5d^1$ transition fo teh Ce^{3+} ion. Samples of CeL^4, CeL^8 and CeL^{12} complexes were prepared in varying concentrations of acid (0.5 to 3.0 M HCl) such that the total ionic strength ([KCl] + [HCl]) was maintain at 3.0 M in each sample. The Ce^{3+} absorbance at 324 nm was then measured as a function of time. Under these conditions the pseudo-first-order rate constant, characterizing the dissociation rate (k_d) arises from two dissociation mechanisms: the spontaneous dissociation of the metal ion characterized by the rate constant, k_0, and the proton assisted dissociation characterized by the rate constant, k_1. The two mechanisms are related according to equation 4

$$k_d = k_0 + k_1[H^+] \quad (4)$$

Plotting the observed dissociation rates, k_d, as a function of acid concentration afforded straight lines from which the values of k_0 and k_1 were determined for each complex (Table 3). When these dissociation rate constants, k_0 and k_1, are compared with the log K_{ML} values determined for DOTA-tetramide complexes (Table 2 and Table 3) the two measures of stability are found to correlate closely: the higher the thermodynamic stability constant of a complex the smaller both the spontaneous and acid-catalyzed dissociation rate constants. However, this correlation between kinetic and thermodynamic stability no longer holds true if the ligating groups of the pendant arm are changed from amides to acetates. CeDOTA, with four acetate pendant arms, has much higher thermodynamic stability than any of the DOTA-tetaramide complexes and

this may well result in the apparent absence of spontaneous dissociation in this system. However, the rate constant for acid-catalyzed dissociation (k_1) is much larger than those observed for the DOTA-tetraamide complexes (except CeL^{12}) because coordinated acetates, unlike coordinated amides can be protonated in acidic media resulting in dissocation of the pendant arms.

As with the thermodynamic stability measurements L^{12} behaved unusually in these experiments. Fitting the data obtained for CeL^{12} afforded a large negative value of k_0 with large uncertainty, suggesting that either spontaneous dissociation does not occur in the case of CeL^{12} or that a different mechanism of dissociation may occur under mildly acidic conditions ($[H^+] < 0.25$ M). It also must be emphasized here, that the k_0 values are determined by linear extrapolation which is known to provide good results only when it is used to not too far beyond the known data range. Additionally, the dissociation of the complex may take place by entirely different mechanism when moving form 1.0 – 2.0 M acid concentration to the acid concentration ranged 0.25 M. The acid-catalyzed dissociation constant, k_1, for CeL^{12} was also found to be much larger, more than 3 times larger, than that of even CeDOTA. Clearly this is not a desirable attribute of a complex postulated for use in vivo; however, it is important to consider that acid catalyzed dissociation is of much less concern under the mildly basic conditions that prevail *in vivo*. Perhaps of greater importance in vivo is the rate of spontaneous dissociation which was observed for all DOTA-tetraamide complexes (except L^{12}) but not for DOTA. Furthermore other mechanisms of complex dissociation are believed to occur *in vivo* including: trans-metallation, particularly with Zn^{2+} and Cu^{2+}, and ligand transfer reactions. Indeed, it is widely believed that trans-metallation with Zn^{2+} is the most important mechanism contributing to the release of Ln^{3+} ions from their complexes *in vivo*.

The interplay of endogenous ligands and metal ions and their effect on metal complex dissociation in a biological milieu is complicated and near impossible to mimic *in vitro*. We therefore set out to assess the stability of these lanthanide complexes in biological media by assessing their stability in serum and evaluating their tissue distribution in normal mice. A number of lanthanide radioisotopes are available but ^{177}Lu ($t_{1/2}$ = 6.62 days; β^-: 0.498 MeV, 78.6%; γ: 208 KeV, 11 %) has shown versatility in both imaging and radiotherapy applications due to its relatively low energy γ photons and β^- emissions [20]. The ligands L^1, L^2, L^4 L^8 and L^{12} were successfully labelled with ^{177}Lu under no carrier added (n.c.a.) or carrier added (c.a.) conditions with $^{177}LuCl_3$ in ammonium acetate buffer (pH 6.5, 2 h) (Table 4). Radiochemical yields were determined by radio-TLC and conversions found to be quantitative in each case. An aliquot (10 μL) of each ^{177}LuL complex was added to rat serum (100 μL) and the sample was incubated at 37 °C to assess the serum stability of the ^{177}LuL complex. The complex concentration in these experiments was in the range 0.33 – 0.83 mM. Samples of the complex in rat serum were analysed by radio-TLC after 24 hours and the activity at the known R_f of the complex was then compared with the total activity in all other regions of the TLC plate. It was assumed that the intact complex would exhibit the known R_f of the complex and that any activity from other parts of the plate corresponded to metal that had dissociated from the ligand. $^{177}LuL^1$, $^{177}LuL^2$, $^{177}LuL^4$, and $^{177}LuL^8$ were all found to be resistant to dissociation in serum under the conditions of this experiment with no evidence of free ^{177}Lu observed, Table 4. This indicates that the high kinetic *in vitro* stability of these complexes (vide supra) transfers to the ex vivo serum environment and furthermore suggests that these complexes are indeed stable enough for use in vivo. The octanol/water partition coefficient (log *P*, octanol/water) data (Table 4) demonstrate that the additional peripheral hydroxyl groups on LuL^{12} impart increased hydrophilicity with respect to LuL^4 and LuL^8.

Biodistribution Studies

The distribution of a chelate at different times post-injection also provides some insight into complex stability *in vivo*. Lanthanide ions liberated from the complex are known to accumulate in teeth and bone [21,22] but are also taken up by liver and spleen as aggregates of the lanthanide ions with native proteins as they are cleared through the hepatobiliary and reticuloendothelial systems [23]. The biodistribution profiles of $^{177}LuL^{1}$, $^{177}LuL^{2}$, $^{177}LuL^{4}$, $^{177}LuL^{8}$ and $^{177}LuL^{12}$ (n.c.a.; typical dose ~ 0.3 μmol kg^{-1}) were measured in balb/c mice by administering the complex in a PBS buffer via tail vein injection (typical dose ~ 0.3 μmol kg^{-1}). The animals were sacrificed at 0.5, 1, 4 and 24 hours post-injection and organs of interest excised, weighed and the activity counted. The biodistribution data are summarized in Table 5 (%ID/g) and Table 3S (%ID/organ)..

All five compounds were cleared largely by kidney filtration (> 90%) within 1 hour of administration. It has been reported that negatively charged copper complexes derived from tetraaza-macrocycles are cleared through the kidneys more efficiently than their positively charged counterparts [24]. Although the four positively charged complexes, $^{177}LuL^{1}$, $^{177}LuL^{4}$, $^{177}LuL^{8}$, and $^{177}LuL^{12}$ are cleared effectively by the renal system they are retained in the kidney rather longer than the negatively charged, $^{177}LuL^{2}$ complex [25]. Over the course of the first hour post-injection, the four positively charged complexes showed significantly ($p < 0.05$) higher uptake than $^{177}LuL^{2}$ in the major organs (blood, liver, spleen, kidneys and lungs), the notable exception being muscle, for which both $^{177}LuL^{2}$ and $^{177}LuL^{12}$ exhibited markedly higher uptake than the other chelates in this study. Over a longer time period, however, all five complexes studied here exhibited rapid clearance from the major organs with low residual activity observed at 4 and 24 hours post-injection irrespective of overall charge.

Perhaps the most marked difference in tissue distribution was observed in bone uptake of the positively charge complexes. All four positively charged complexes exhibit higher levels of activity in the bone than $^{177}LuL^{2}$ at 0.5 and 1 hour post-injection. Although the free lanthanide ions are known to accumulate in the bone, because the rates of complex dissocation are so slow it is unlikely that elevated activity in bone seen here at the early time points is the result of dissociation of the complex. The activity in the bone decreases quite rapidly and, at 24 hours post-injection, the level of bone activity seen for all five chelates is comparable. This is in stark contrast to free lanthanide ions that gradually build up in bone, increasing activity over time [21]. Secondly the data obtained for liver and spleen is not indicative of dissociation of the complexes [23]. Of the positively charged complexes, $^{177}LuL^{1}$ has significantly higher ($p < 0.05$) liver uptake at both 1 and 4 hours post-injection than those bearing peripheral hydroxyl groups, $^{177}LuL^{4}$, $^{177}LuL^{8}$, and $^{177}LuL^{12}$. The complexes $^{177}LuL^{2}$ and $^{177}LuL^{12}$ showed the lowest levels of liver uptake at 1 hour post-injection. Overall these complexes exhibited low levels of liver uptake indicating that both hepatobiliary clearance and complex dissociation do not occur to a significant extent. The %ID / organ for the spleen is extremely low for all five chelates and, since dissociation of the metal ion would surely lead to elevated activity levels in the spleen, this is a good indication that for each complex, little or no dissociation of the metal ion occurs prior to excretion.

The rate of blood clearance of a chelate is an important pharmacokinetic property. It has previously been reported that the biological half-life of drugs in the blood stream can be increased by incorporating polyethylene glycol groups into the drug [26–29]. Noting the relatively high levels of accumulation of the three complexes bearing peripheral hydroxyl groups ($^{177}LuL^{4}$, $^{177}LuL^{8}$ and $^{177}LuL^{12}$) in blood after 0.5 hours (Table 5), a further study was performed to compare clearance of these chelates from blood over shorter time periods. Samples of blood were taken from mice at 2, 5, 10, 15, 30, 60 and 240 minutes after the administration of $^{177}LuL^{1}$, $^{177}LuL^{4}$, $^{177}LuL^{8}$ and $^{177}LuL^{12}$. The data, summarized in Figure

1, show that the complex bearing a positive charge but no peripheral hydroxyl groups, $^{177}LuL^1$, is cleared from the blood most rapidly while the complex having the largest number of peripheral hydroxyl groups, $^{177}LuL^{12}$, clears most slowly.

A two-compartment open model [30] was used to calculate the *in vivo* pharmacokinetic parameters: $t_{1/2\alpha}$, $t_{1/2\beta}$ and $AUC_{0\rightarrow\infty}$ (Table 6). While the distribution half-lives ($t_{1/2\alpha}$) of the four positively charged complexes were similar (8.7 – 10.6 min), the elimination half-lives ($t_{1/2\beta}$) and $AUC_{0\rightarrow\infty}$ values correlated with the number of peripheral hydroxyl groups in each complex.

The MRI contrast media used in clinical practice today (Chart 1) are administered in high doses (0.1 mmolkg^{-1}), three orders of magnitude greater than the doses employed in these biodistribution experiments. PARACEST agents, which are currently limited by their relative lack of sensitivity relative to Gd^{3+}-based agents, may require even higher doses although future improvements in sensitivity will almost certainly to reduce these dosing requirements. Such high doses can overwhelm transport pathways in the body, significantly altering the biodistribution profiles [21]. It has recently been reported that some tri-cationic DOTA-tetraamide complexes are acutely toxic in rodents at these high dose levels [8]. In order to assess the effect of this increased dose, injections of all five chelates were formulated with carrier added. A solution of $^{177}LuCl_3$ was added to cold $LuCl_3$ (carrier) prior to addition of the ligand, which was slightly in excess (1.2 eq) relative to the total concentration of Lu^{3+}, to form a carrier-added ^{177}Lu labelled complex so that when administered at 0.1 mmolkg^{-1} it would only administer the same level of radiation as in the previous experiment.

No toxic effects were observed for any of the chelates when low doses of n.c.a complexes (0.3 μmolkg^{-1}) were administered. In contrast, animals administered with c.a. complexes of LuL^1, LuL^4 and LuL^8 (total [Lu^{3+}]: 0.1 mmolkg^{-1}) showed signs of distress immediately post-injection and expired within 5 minutes. Given the slow rate of complex dissociation established both in vitro and in serum, death occurs too rapidly to be the result of dissociation of the complex and must be the result of an inherent toxicity of these tri-cationic complexes, consistent with our earlier report [8]. The cause of death was previously postulated to involve an interaction between the complex and heart tissue that caused a rapid weakening of the heart beat [8]. It is well known that cells can be more efficiently penetrated by positively charged agents [31] because of positive charge facilitated internalization and this may be the root of their effect on the heart and their subsequent toxicity.

In sharp contrast, neither LuL^2 nor LuL^{12} was observed to cause any appreciable toxic effects over the entire 48 hour observation period. This result was anticipated for the negatively charged LuL^2 complex which had previously been administered to rodents at typical MRI doses [8]. It was more surprising in the case of LuL^{12} complex which probably retains some level of positive charge, despite the apparent presence of relatively acidic amide or hydroxyl protons that may reduce the overall charge somewhat. To our knowledge LuL^{12} is the first example of a positively charged lanthanide DOTA-tetraamide complex that is not toxic when administered at a typical MRI dose. While the precise reasons for this absence of acute toxicity at 0.1 mmolkg^{-1} are uncertain, one can draw an analogy between the complexes LuL^1, LuL^4 LuL^8 and LuL^{12}, and the clinically approved MRI contrast agents GdHP-DO3A and GdDO3A-butrol (Chart 1). GdHP-DO3A and GdDO3A-butrol are structurally analogous with the Gd^{3+} ion coordinated by the macrocyclic ring, three acetate pendant arms and one ethyl-hydroxyl group. The only difference between the two complexes is the substitution of the methyl substituent of the hydroxyl pendant arm of HP-DO3A for an ethanediol in DO3A-butrol. This small change, incorporating two peripheral hydroxyl groups in DO3A-butrol, has a significant effect on the LD_{50} of the complexes, increasing from 12 mmolkg^{-1} for GdHP-DO3A to 23 mmolkg^{-1} for GdDO3A-butrol [32]. Since this decrease in toxicity can only be ascribed to the

introduction of the peripheral hydroxyl groups, we suggest that excess hydroxyl groups in LuL^{12} render this complex less toxic, even at the doses required for MRI.

Tissue distribution profiles of carrier added LuL^{12} in normal balb/c mice were determined at 4, 24, and 48 hour post-injection. For comparative purposes, the biodistribution profiles of n.c.a. and c.a. are presented together in Table 7. In general, when the complex is administered at the higher dose, a greater uptake by the major organs is observed. The complex is primarily cleared *via* the renal system with minimal soft tissue activity detected at 48 hours post-injection, whereas a significant uptake increase ($p < 0.05$) was observed in the bone from 24 to 48 hours. Interestingly at the higher dose the complex exhibited significantly lower kidney uptake ($p < 0.05$) than at the lower dose within 4 hours post-injection. This is likely due to the presence of a scavenger receptor, megalin, in the proximal tubes of the kidneys that is responsible for the endocytosis of molecules passing through the kidneys [33]. If this scavenger receptor is exposed to a large amount of the complex shortly after injection it is likely to become saturated and this would result in the lower kidney uptake of the complex at the higher dose.

Conclusions

The general rule of thumb for identifying a “stable” lanthanide contrast agents has been associated with the concept of the highest thermodynamic stability. Indeed this is an important consideration; however, the influence of kinetic inertness should not be underestimated. In the present study we have demonstrated that a cationic lanthanide chelate ($^{177}LuL^{12}$) possessing unremarkable thermodynamic stability can be tolerated at the typical MR contrast agent dosage. Furthermore, the biodistribution profiles for this series of DOTA-tetraamide complexes bearing peripheral hydroxyl groups are quite similar to anionic chelates such as Dotarem which is accepted as safe for human use. The Ln^{3+} complexes of the three DOTA-tetraamide ligands were evaluated with respect to thermodynamic and kinetic properties and the data acquired for complexes of L^4 and L^8 was similar to those obtained for other DOTA-tetraamide complexes. The data acquired for L^{12} is less easily understood; nonetheless the *in vivo* results are significant and indicate that sufficient peripheral hydroxyl functionalization can be used to mask and control undesirable feature of the chelate. Finally, the utility of DOTA-tetramide ligands are not limited to PARACEST applications. These ligands can also be modified to include bifunctional linkers enabling covalent attachment to targeting vectors. In this manner the desirable kinetic properties of these unique ligands can further extend their applications to other modalities such as nuclear medicine or imaging.

Supplementary Material

Refer to Web version on PubMed Central for supplementary material.

Acknowledgments

The authors thank the National Institutes of Health (RR-02584, CA-126608, CA119219 and CA-115531) and the Robert A Welch Foundation (AT-584) for financial assistance. Xiankai Sun also acknowledges the support of his start-up funds provided by the Harold C. Simmons Comprehensive Cancer Center and the Department of Radiology of UT Southwestern Medical Center at Dallas.

References

1. Caravan P, Ellison JJ, McMurry TJ, Lauffer RB. Chem Rev 1999;99(9):2293–2352. [PubMed: 11749483]
2. Toth, E.; Merbach, AE. Chemistry of Contrast Agents in Medical Magnetic Resonance Imaging. New York: Wiley; 2001.
3. Woods M, Woessner DE, Sherry AD. Chem Soc Rev 2006;35(6):500–511. [PubMed: 16729144]

4. Aime S, Barge A, Batsanov AS, Botta M, Castelli DD, Fedeli F, Mortillaro A, Parker D, Puschmann H. Chem Commun 2002;(10):1120–1121.
5. Pasha A, Tircso G, Benyo ET, Brucher E, Sherry AD. Eur J Inorg Chem 2007;(27):4340–4349. [PubMed: 19802361]
6. Baranyai Z, Brucher E, Ivanyi T, Kiraly R, Lazar I, Zekany L. Helv Chim Acta 2005;88(3):604–617.
7. Kalman FK, Woods M, Caravan P, Jurek P, Spiller M, Tircso G, Kiraly R, Brucher E, Sherry AD. Inorg Chem 2007;46(13):5260–5270. [PubMed: 17539632]
8. Woods M, Caravan P, Geraldes CFGC, Greenfield MT, Kiefer GE, Lin M, McMillan K, Prata MIM, Santos AC, Sun X, Wang J, Zhang S, Zhao P, Sherry AD. Invest Radiol. 2008 In Press.
9. Woods M, Pasha A, Kiefer GE, Woessner DE, Sherry AD. 2008 Unpublished results.
10. Irving HM, Miles MG, Pettit LD. Anal Chim Acta 1967;38(4):475.
11. Zékány, L.; Nagypál, I. Chapter. In: Legett, DJ., editor. Computational Methods for Determination of Formation Constants. New York: Plenum Press; 1985.
12. Martell, AE.; Smith, RM.; Motekaitis, RJ. Critically Selected Stability Constants of Metal Complexes Database Version 8.0. Texas A&M University; 2004.
13. Baes, CFJ.; Mesmer, RE. The Hydrolysis of Cations. New York: John Wiley & Sons Inc; 1976.
14. Chaves S, Delgado R, Da Silva JJRF. Talanta 1992;39(3):249–254. [PubMed: 18965370]
15. Delgado R, da Silva JJRF. Talanta 1982;29(10):815–822. [PubMed: 18963244]
16. Kumar K, Tweedle MF, Malley MF, Gougoutas JZ. Inorg Chem 1995;34(26):6472–6480.
17. Woods M, Kovacs Z, Kiraly R, Brucher E, Zhang S, Sherry AD. Inorg Chem 2004;43(9):2845–2851. [PubMed: 15106971]
18. Cacheris WP, Nickle SK, Sherry AD. Inorg Chem 1987;26(6):958–960.
19. Brücher E, Laurenczy G, Makra ZS. Inorg Chim Acta 1987;139(1–2):141–142.
20. Li WP, Ma DS, Higginbotham C, Hoffman T, Ketring AR, Cutler CS, Jurisson SS. Nucl Med Biol 2001;28(2):145–154. [PubMed: 11295425]
21. Wedeking P, Kumar K, Tweedle MF. Nucl Med Biol 1993;20(5):679–691. [PubMed: 8358355]
22. Wedeking P, Tweedle M. Nucl Med Biol 1988;15(4):395–402.
23. Arvela P. Prog Pharma 1979;2(3):69–114.
24. Jones-Wilson TM, Deal KA, Anderson CJ, McCarthy DW, Kovacs Z, Motekaitis RJ, Sherry AD, Martell AE, Welch MJ. Nucl Med Biol 1998;25(6):523–530. [PubMed: 9751418]
25. Melis M, Krenning EP, Bernard BF, Barone R, Visser TJ, Jong M. Eur J Nucl Med Mol Imaging 2005;32(10):1136–1143. [PubMed: 15912401]
26. Klibanov AL, Maruyama K, Torchilin VP, Huang L. FEBS Lett 1990;268(1):235–237. [PubMed: 2384160]
27. Sun X, Rossin R, Turner JL, Becker ML, Joralemon MJ, Welch MJ, Wooley KL. Biomacromolecules 2005;6(5):2541–2554. [PubMed: 16153091]
28. Lukyanov AN, Hartner WC, Torchilin VP. J Controlled Release 2004;94(1):187–193.
29. Trubetskoy VS, Torchilin VP. Adv Drug Deliv Rev 1995;16(23):311–320.
30. Welling, PG. Pharmacokinetics: Processes, Mathematics, and Applications. Vol. Second Edition. Washington D.C: American Chemical Society; 1997.
31. Deshayes S, Morris MC, Divita G, Heitz F. Cellular Mol Life Sci 2005;62(16):1839–1849. [PubMed: 15968462]
32. Vogler H, Platzek J, Schuhmann-Giampieri G, Frenzel T, Weinmann H-J, Raduchel B, Press W-R. Eur J Rad 1995;21(1):1–10.
33. de Jong M, Barone R, Krenning E, Bernard B, Melis M, Visser T, Gekle M, Willnow TE, Walrand S, Jamar F, Pauwels S. J Nucl Med 2005;46(10):1696–1700. [PubMed: 16204720]

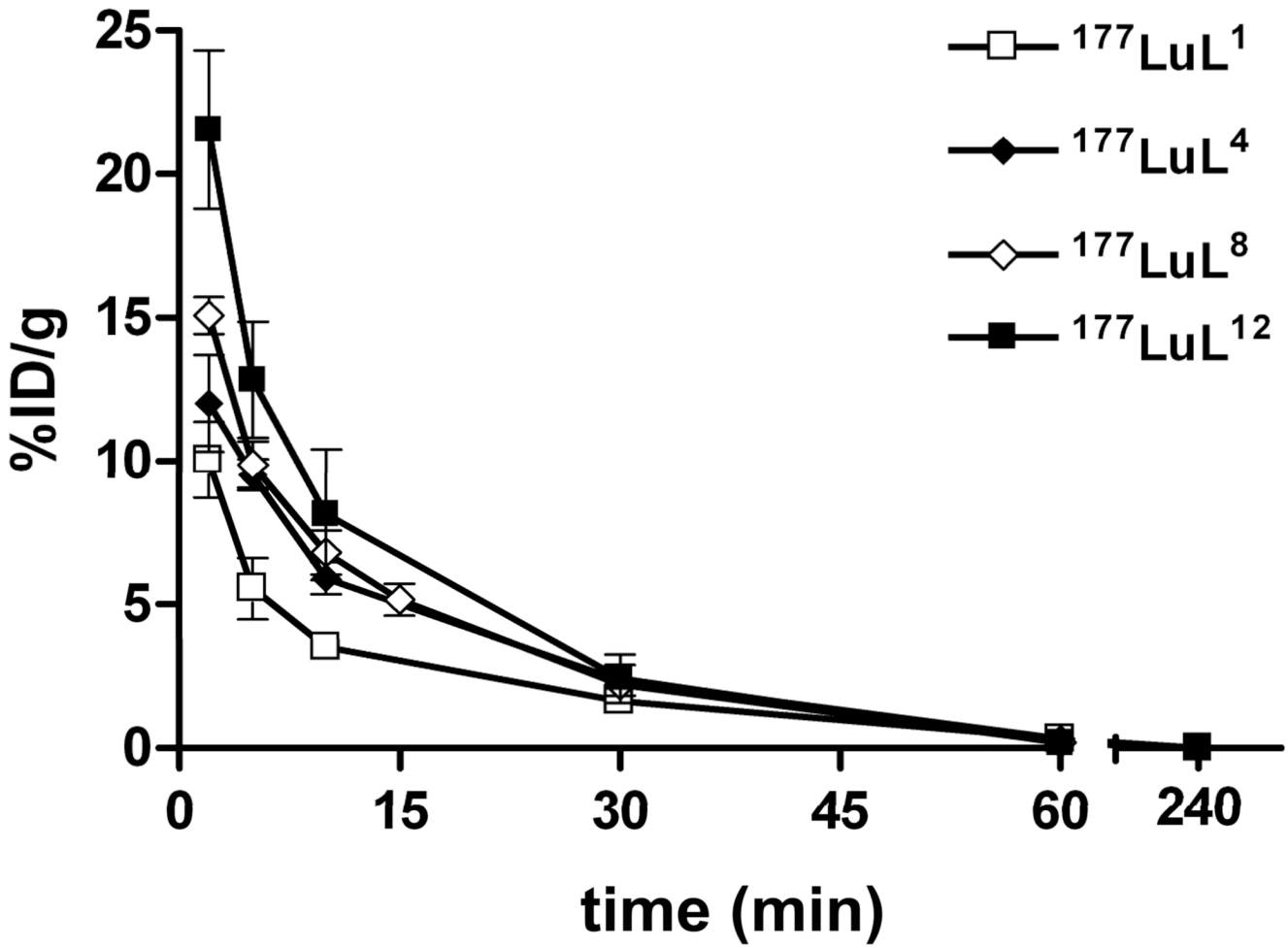

Figure 1.
Comparative time-activity curves of ^{177}Lu-labeled complexes in the blood of balb/c mice (n = 4).

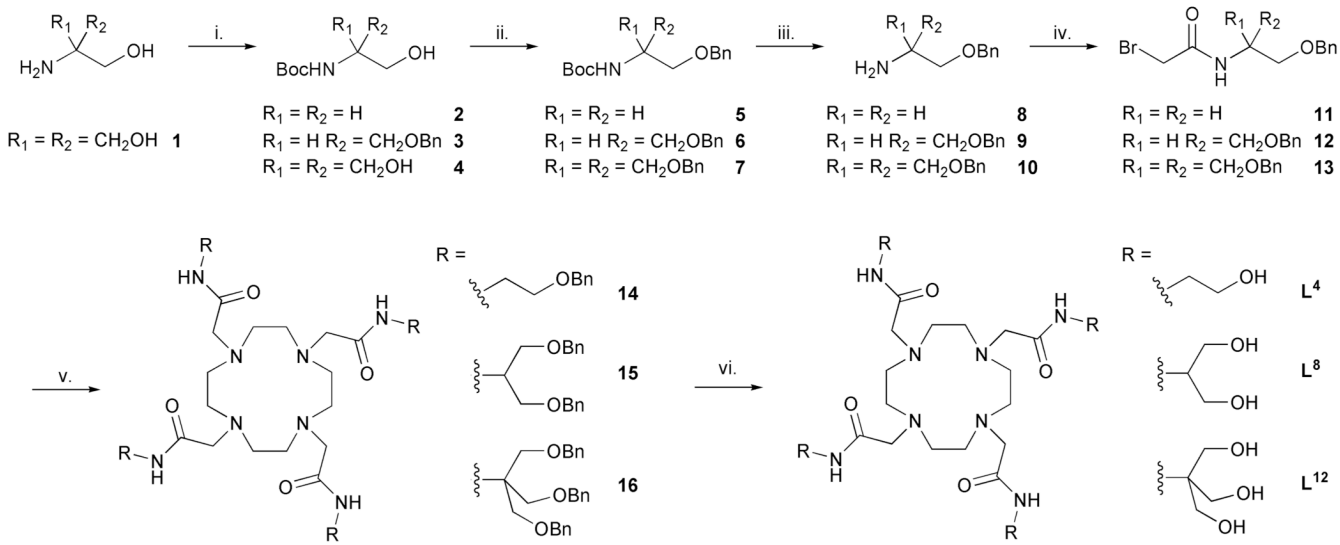

Scheme 1.

The synthesis of the hydoxylated DOTA-tetraamide ligands. *Reagents and conditions* i. $(^{t}BuOCO)_2O$ / MeOH / $^{t}BuOH$; ii. BnBr / KOH / DMF / RT; iii. CF_3CO_2H / CH_2Cl_2; iv. $BrCH_2COBr$ / K_2CO_3 / CH_2Cl_2 / 0 °C; v. cyclen / base / MeCN / 60 °C; vi. $Pd(OH)_2$ on C / H_2 / CH_3CO_2H / MeOH.

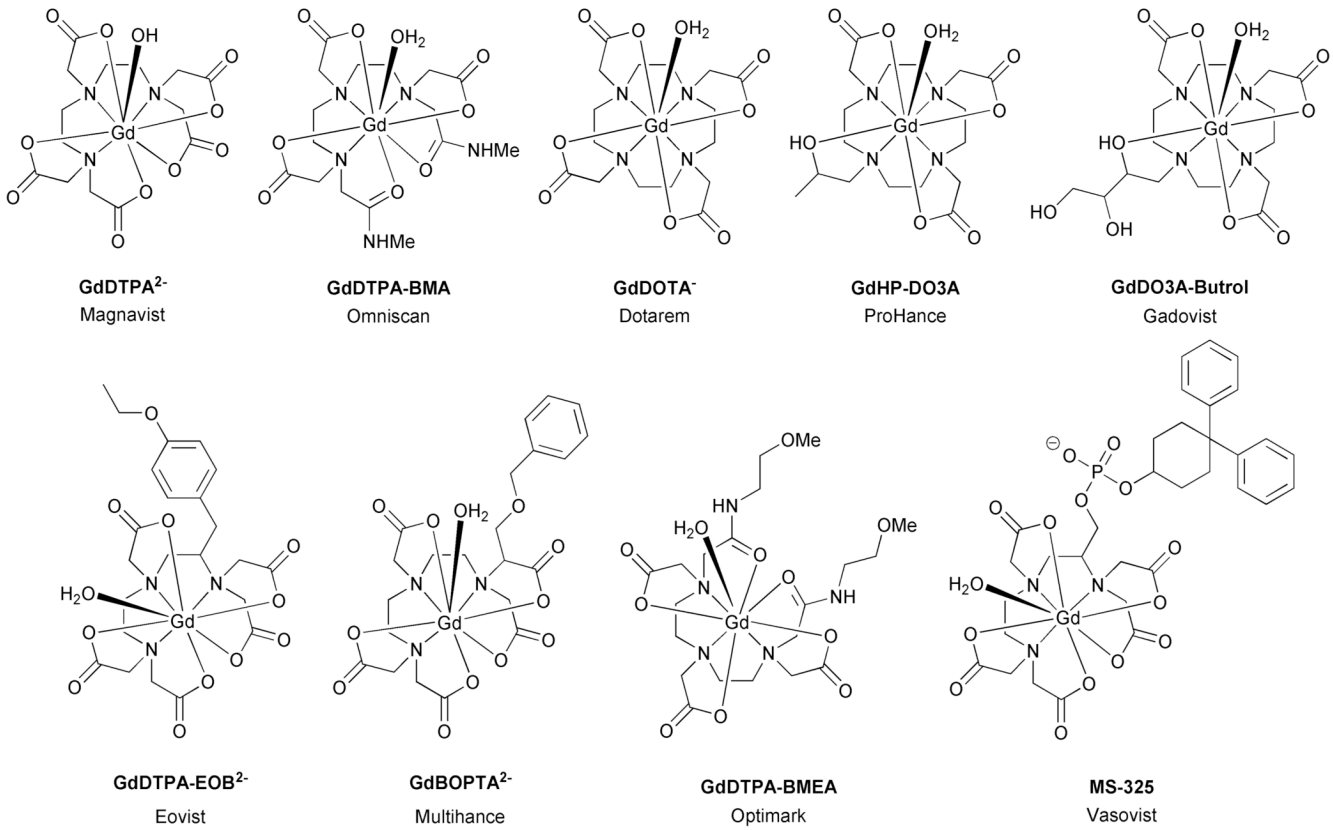

Chart 1.
Clinically approved Gd^{3+}-based MRI contrast agents

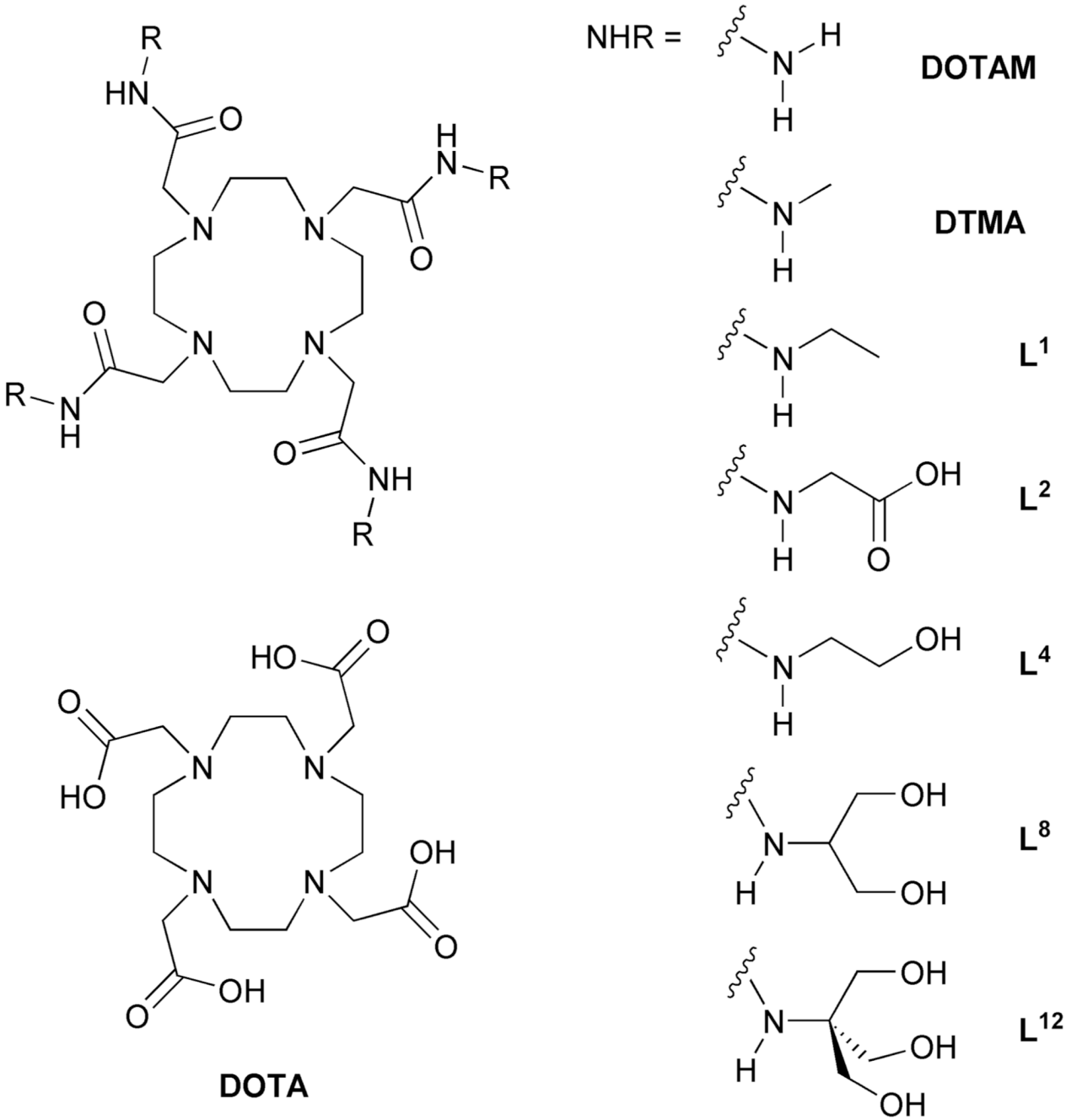

Chart 2.
The structures of DOTA-tetraamide ligands, potential PARACEST agents

Table 1

The protonation constants ($log\ K_i$) of selected DOTA-tetraamide ligands and the thermodynamic stability constants ($log\ K_{ML}$) of their complexes with endogenous divalent metal ions (M^{2+}) (I = 1.0 M KCl, 25°C).

	DOTAM[a]	DTMA[a]	L[1][a]	L[2][b]	L[4]	L[8]	DOTA[c]
Protonation constants							
$log\ K_1^H$	9.08	9.56	9.33	9.19	8.69 ± 0.01	8.43 ± 0.01	12.60
$log\ K_2^H$	6.20	5.95	6.39	6.25	6.57 ± 0.01	6.94 ± 0.01	9.70
$log\ K_3^H$	-	-	-	4.08	-	-	4.50
$log\ K_4^H$	-	-	-	3.45	-	-	4.14
$log\ K_5^H$	-	-	-	3.20	-	-	2.32
$log\ K_6^H$	-	-	-	1.40	-	-	-
Stability constants							
$log\ K_{MgL}$	4.65	4.33	4.49	4.34	4.47 ± 0.01	4.86 ± 0.01	11.15
$log\ K_{CaL}$	10.32	10.11	10.74	10.39	9.89 ± 0.01	10.34 ± 0.01	16.37
$log\ K_{CuL}$	14.50	14.61	16.40	13.39	14.83 ± 0.02	14.68 ± 0.03	22.72
$log\ K_{ZnL}$	13.77	13.66	16.55	-	15.00 ± 0.02	14.35 ± 0.02	18.17

[a] from reference [5],

[b] from reference [18],

[c] from references [14–16].

Table 2

Thermodynamic stability constants (*log* K_{ML}) of DOTA-tetraamide complexes of several trivalent lanthanide ions (Ln^{3+}) (*I* = 1.0 M KCl, 25°C).

Ln^{3+}	DOTAM[a]	DTMA[a]	L^1[a]	L^2[b]	L^4	L^8	DOTA[b]
Ce^{3+}	11.93	12.68	13.0	13.02	12.01 ± 0.07	11.90 ± 0.12	23.4
Nd^{3+}	12.40	13.08	14.37	14.45	12.95 ± 0.08	12.66 ± 0.22	23.0
Eu^{3+}	13.80	13.67	15.09	14.84	13.41 ± 0 .09	13.18 ± 0.11	23.5
Dy^{3+}	13.57	13.84	15.09	14.37	12.91 ± 0.24	12.98 ± 0.07	24.8
Yb^{3+}	-	-	-	14.25	13.07 ± 0.12	12.77 ± 0.08	25.0
Lu^{3+}	13.53	13.91	14.62	-	12.21 ± 0.04	12.20 ± 0.08	25.4

a) from reference [5],

b) from reference [18].

Table 3

Proton assisted dissociation rates for Ce^{3+} complexes of DOTA and selected DOTA-tetraamides.

Ligand	k_0 (s^{-1})	k_1 ($M^{-1}s^{-1}$)
DTMA[a]	1.1×10^{-5}	2.6×10^{-5}
L^4	$(7.8 \pm 0.4) \times 10^{-5}$	$(1.26 \pm 0.02) \times 10^{-4}$
L^8	$(9.6 \pm 0.4) \times 10^{-5}$	$(1.08 \pm 0.02) \times 10^{-4}$
L^{12}	—[b]	$(3.1 \pm 0.1) \times 10^{-3}$
DOTA[c]	n.d.	8×10^{-4}

a) from reference [5];

b) the large negative value may be explained by a different mechanism accessible for dissociation at lower acid concentrations;

c) from reference [19].

Table 4

Reaction conditions for the formation of ^{177}Lu-labeled complexes and their partition coefficients and *in vitro* serum stability.

Complex	Reaction conditions	Radiochem. purity (%)	R_f	logP^c	Serum stability at 24 h (% intact)
^{177}LuL^1	n.c.a: 0.1 M NH_4OAc pH 6.5 2 h at 60 °C	100 (n.c.a.)	0.41[a]	3.54 ± 0.42	100
^{177}LuL^2		100 (n.c.a.)	0.21[b]	5.23 ± 0.27	100
^{177}LuL^4		100 (n.c.a.)	0.74[a]	3.55 ± 0.27	100
^{177}LuL^8	c.a.: 1.2:1 ligand/lutetium 0.1 M NH_4OAc pH 6.5 2 h at 60 °C	100 (n.c.a.)	0.79[a]	3.52 ± 0.43	100
^{177}LuL^{12}		100 (n.c.a.)	0.80[a]	3.98 ± 0.23	100
^{177}LuL^{12}		100 (c.a.)	0.82[a]	n.d.	n.d.

n.d.: not determined

c.a.: carrier added

n.c.a.: no carrier added

[a] RP-18; 1:1 methanol/10% ammonium acetate

[b] RP-18; 1:9 methanol/10% ammonium acetate

[c] Determined in n-octanol/H_2O.

Table 5

Biodistribution of 0.3 μmolkg^{-1} doses of ^{177}Lu complexes in normal Balb/c mice (n = 4). Data are presented as %ID/g ± standard deviation.

		Time points (h)			
Complex	**Tissue**	**0.5**	**1**	**4**	**24**
^{177}LuL^{1}	Blood	1.64 ± 0.28	0.33 ± 0.11	0.01 ± 0.00	0.00 ± 0.00
	Lung	1.86 ± 0.20	0.69 ± 0.12	0.16 ± 0.06	0.06 ± 0.01
	Liver	0.67 ± 0.07	0.34 ± 0.05	0.23 ± 0.04	0.12 ± 0.02
	Spleen	0.59 ± 0.05	0.25 ± 0.09	0.10 ± 0.05	0.07 ± 0.03
	Kidney	5.75 ± 1.29	3.46 ± 0.37	3.12 ± 0.08	1.21 ± 0.28
	Heart	0.75 ± 0.04	0.22 ± 0.02	0.06 ± 0.01	0.05 ± 0.04
	Muscle	0.50 ± 0.10	0.41 ± 0.12	0.09 ± 0.04	0.02 ± 0.02
	Fat	0.27 ± 0.03	0.18 ± 0.12	0.03 ± 0.00	0.02 ± 0.01
	Bone	1.54 ± 1.52	0.66 ± 0.18	0.24 ± 0.10	0.09 ± 0.03
^{177}LuL^{2}	Blood	0.53 ± 0.24	0.08 ± 0.05	0.03 ± 0.00	0.01 ± 0.00
	Lung	1.38 ± 0.47	0.12 ± 0.04	0.07 ± 0.02	0.05 ± 0.01
	Liver	0.44 ± 0.13	0.10 ± 0.02	0.09 ± 0.02	0.05 ± 0.01
	Spleen	0.46 ± 0.19	0.10 ± 0.06	0.07 ± 0.03	0.06 ± 0.03
	Kidney	5.06 ± 1.84	1.91 ± 0.21	1.58 ± 0.27	0.68 ± 0.05
	Heart	0.56 ± 0.23	0.07 ± 0.02	0.03 ± 0.03	0.04 ± 0.02
	Muscle	1.43 ± 0.25	0.12 ± 0.03	0.07 ± 0.05	0.04 ± 0.02
	Fat	0.32 ± 0.10	0.07 ± 0.01	0.06 ± 0.04	0.03 ± 0.01
	Bone	0.07 ± 0.04	0.01 ± 0.00	0.01 ± 0.00	0.18 ± 0.11
^{177}LuL^{4}	Blood	2.35 ± 0.53	0.31 ± 0.18	0.01 ± 0.00	0.00 ± 0.00
	Lung	2.33 ± 0.44	0.47 ± 0.23	0.07 ± 0.00	0.07 ± 0.05
	Liver	0.66 ± 0.16	0.24 ± 0.07	0.12 ± 0.02	0.26 ± 0.03
	Spleen	0.70 ± 0.14	0.18 ± 0.08	0.10 ± 0.04	0.07 ± 0.07
	Kidney	7.98 ± 1.70	3.26 ± 0.33	1.87 ± 0.31	1.63 ± 0.32
	Heart	0.94 ± 0.26	0.17 ± 0.02	0.05 ± 0.01	0.52 ± 0.03
	Muscle	0.66 ± 0.05	0.31 ± 0.14	0.03 ± 0.01	0.06 ± 0.03

		Time points (h)			
Complex	**Tissue**	**0.5**	**1**	**4**	**24**
	Fat	0.32 ± 0.05	0.32 ± 0.06	0.01 ± 0.01	0.01 ± 0.01
	Bone	1.58 ± 0.39	0.71 ± 0.38	0.14 ± 0.08	0.08 ± 0.05
$^{177}LuL^{8}$	Blood	2.19 ± 0.32	0.21 ± 0.03	0.01 ± 0.00	0.00 ± 0.00
	Lung	2.17 ± 0.28	0.46 ± 0.05	0.22 ± 0.19	0.07 ± 0.03
	Liver	0.63 ± 0.10	0.24 ± 0.04	0.15 ± 0.06	0.10 ± 0.02
	Spleen	0.98 ± 0.43	0.17 ± 0.04	0.09 ± 0.03	0.13 ± 0.03
	Kidney	6.34 ± 0.79	3.41 ± 0.49	2.28 ± 0.67	1.46 ± 0.23
	Heart	0.98 ± 0.14	0.20 ± 0.08	0.03 ± 0.01	0.05 ± 0.03
	Muscle	0.60 ± 0.18	0.38 ± 0.19	0.03 ± 0.02	0.02 ± 0.01
	Fat	0.34 ± 0.16	0.14 ± 0.07	0.02 ± 0.00	0.05 ± 0.03
	Bone	1.32 ± 0.44	0.38 ± 0.17	0.12 ± 0.06	0.13 ± 0.02
$^{177}LuL^{12}$	Blood	2.42 ± 0.85	0.19 ± 0.07	0.01 ± 0.00	0.01 ± 0.00
	Lung	2.28 ± 0.81	0.48 ± 0.30	0.07 ± 0.04	0.08 ± 0.03
	Liver	0.78 ± 0.19	0.17 ± 0.02	0.13 ± 0.01	0.12 ± 0.06
	Spleen	0.77 ± 0.19	0.15 ± 0.08	0.05 ± 0.05	0.07 ± 0.02
	Kidney	7.99 ± 0.86	3.13 ± 0.40	2.62 ± 0.33	1.15 ± 0.12
	Heart	0.92 ± 0.19	0.12 ± 0.06	0.03 ± 0.02	0.06 ± 0.02
	Muscle	2.23 ± 0.74	0.13 ± 0.07	0.03 ± 0.01	0.03 ± 0.01
	Fat	0.64 ± 0.25	0.09 ± 0.03	0.03 ± 0.02	0.04 ± 0.02
	Bone	1.52 ± 0.43	0.36 ± 0.17	0.13 ± 0.05	0.09 ± 0.04

Table 6

Pharmacokinetic parameters of ^{177}Lu labeled complexes in normal balb/c mice.

Complex	$t_{1/2\alpha}$ (min)	$t_{1/2\,\beta}$ (min)	$AUC_{0\rightarrow\infty}$ (%ID•min/g)
^{177}LuL^{1}	9.7 ± 0.2	27.6 ± 6.5	152 ± 36
^{177}LuL^{4}	10.6 ± 0.4	30.9 ± 1.5	218 ± 56
^{177}LuL^{8}	9.8 ± 0.8	34.8 ± 9.8	235 ± 39
^{177}LuL^{12}	8.7 ± 1.2	35.8 ± 6.9	273 ± 94

Table 7

Comparative biodistribution data of $^{177}LuL^{12}$ formed in normal Balb/c mice (n = 4) administered at doses of 0.3 μmolkg^{-1} (n.c.a.) and 0.1 mmolkg^{-1} (c.a.), respectively. Data are presented as %ID/g ± s.d.

Tissue		4 h	24 h	48 h
Blood	n.c.a.	0.01 ± 0.00	0.01 ± 0.00	0.00 ± 0.00
	c.a.	0.02 ± 0.01	0.00 ± 0.00	0.01 ± 0.01
Lung	n.c.a.	0.07 ± 0.04	0.08 ± 0.03	0.04 ± 0.03
	c.a.	0.15 ± 0.03	0.22 ± 0.09	0.24 ± 0.14
Liver	n.c.a.	0.13 ± 0.01	0.12 ± 0.06	0.05 ± 0.01
	c.a.	0.33 ± 0.06	0.27 ± 0.04	0.21 ± 0.06
Spleen	n.c.a.	0.05 ± 0.05	0.07 ± 0.02	0.56 ± 0.02
	c.a.	0.09 ± 0.05	0.16 ± 0.06	0.25 ± 0.09
Kidney	n.c.a.	2.62 ± 0.33	1.15 ± 0.12	0.63 ± 0.15
	c.a.	1.56 ± 0.13	1.93 ± 0.43	0.60 ± 0.03
Heart	n.c.a.	0.03 ± 0.02	0.06 ± 0.02	0.01 ± 0.00
	c.a.	0.09 ± 0.06	0.05 ± 0.03	0.08 ± 0.03
Muscle	n.c.a.	0.03 ± 0.01	0.03 ± 0.01	0.01 ± 0.00
	c.a.	0.06 ± 0.0	0.06 ± 0.03	0.05 ± 0.02
Fat	n.c.a.	0.03 ± 0.02	0.04 ± 0.02	0.01 ± 0.00
	c.a.	0.05 ± 0.02	0.01 ± 0.00	0.00 ± 0.00
Bone	n.c.a.	0.13 ± 0.05	0.09 ± 0.04	0.01 ± 0.01
	c.a.	0.51 ± 0.13	0.18 ± 0.04	0.67 ± 0.09